

Genomic profiles and removal mechanisms explain  
the observed stratification of  $\text{Fe}^{2+}$ ,  $\text{NH}_4^+$  and  $\text{Mn}^{2+}$   
removal in rapid sand filters

Nienke Koudijs



# Genomic profiles and removal mechanisms explain the observed stratification of $\text{Fe}^{2+}$ , $\text{NH}_4^+$ and $\text{Mn}^{2+}$ removal in rapid sand filters

By

Nienke Koudijs  
4473299

in partial fulfilment of the requirements for the degree of

Master of Science  
in Life Science & Technology

at the Delft University of Technology,  
to be defended publicly on Monday July 5, 2021 at 10:30 AM

Daily supervisor:	Francesc Corbera Rubio
Thesis committee:	Prof. dr. M.C.M. van Loosdrecht
	Dr. Ir. D. van Halem
	Prof. Dr. P.A.S. Daran-Lapujade
	Dr. M. Laurenzi



# Abstract

Groundwater is an excellent source for the production of drinking water due to its low concentration of microorganisms and contaminants. The main contaminants present in groundwater are iron, ammonium and manganese, which are sequentially removed in rapid sand filters by a combination of biological and chemical processes. Currently, limited knowledge of the removal mechanisms challenges the design of new drinking water treatment plants (DWTPs). As a result, different treatment schemes are used to treat groundwater with a similar composition. We hypothesize that the difference in plant configuration does not affect the stratification of removal processes. In the present work, the spatial distribution of taxonomic and functional microbiological profiles and physical-chemical removal mechanisms were investigated in two DWTPs with similar incoming water but different treatment schemes. One plant employs a dual bed filter, while the other uses two sequential filters. Concentration profiles and composition of the coating on the sand showed sequential removal of iron and manganese, while ammonium removal was ubiquitous. Activity batch tests revealed section-specific manganese removal mechanisms: adsorption in the first section and oxidation in the second section. The latter is the dominant process in full-scale filters. Manganese oxidation capacity remained constant over the height of the second section. Contrarily, ammonia removal was highly stratified in there. The highest ammonium removal rates were observed at the top section of the filter. Furthermore, ammonium removal rates were higher in the second section compared to the first one. In accordance, metagenomic analysis revealed higher abundances of nitrifying organisms in the second sections. Besides, co-existence of nitrifiers and iron-oxidizers was observed in the top layer, in contrast to the common opinion that iron removal has to be complete before nitrification can start. We (i) conclude that similar distributions in removal mechanisms and genomic profiles were observed in both DWTPs, regardless of plant configuration, (ii) provide the first holistic quantitative analysis of the biological and chemical reactions in full-scale rapid sand filters and, (iii) to our knowledge, prove for the very first time that iron hydroxides on the sand grains adsorb manganese under aerobic conditions, using both adsorption and desorption tests.

# Acknowledgements

The master thesis has been a journey of almost a year in which I learned an enormous amount of things, on both professional and personal level. This wouldn't have been possible without the people around me.

I would like to thank Francesc, who always inspired and motivated me. I really enjoyed our discussions, where you've always been open to my ideas and thoughts or explain whatever I wouldn't understand. I also really liked to work in the lab together with you. You are a great mentor and gave me the confidence to be more independent and trust my own judgement, but when necessary you also gave me the time and space I needed. I am also thankful for how you showed me the academic world and took me onto (sampling) trips to the drinking water treatment plants and Radboud University.

I would also like to thank Michele, who has been really helpful in supervising the project and the experiments. I want to thank you for the insights you gave me and your endless positivity toward the project. Doris, I would like to thank you for your ideas and the discussions we had about the project. It was also great to be invited to the drinking water meetings and learn about completely different parts of the drinking water treatment. Mark, thank you for the help with the project, the discussions and the coffees.

Nina and Simon, I specifically want to thank you for the help with this thesis. Simon, thank you for the help in analysing the coating and all the water samples (800 or so!). Nina, thank you for the help and working together on the metagenomic analysis. I want to thank David C. and Ben for all the help with the DNA extraction. I also want to thank Theo van Alen and Sebastian Lücker for sequencing of the DNA and the extremely helpful discussion about the metagenomic analysis. I would also like to thank Thomas Abeel for the metagenomic insights.

I would also thank the people from Vitens, Jaap Dijkshoorn, Frank Schoonenberg, Martin Vink, Johan Hoentjes and Patrick Teunissen, who made sampling of the filters possible and provide us with a lot of knowledge and information about the plants.

CCCers and drinking water people, thank you for the feedback on the presentations, the input in the project and the coffees and lunches. I would also like to thank the whole EBT group for all the fun, the bbq's, beach volley and just being part of the group.

Ik wil ook mijn familie bedanken voor alle steun en vertrouwen. Papa, mama, Maaïke, Gerben, Yanniek, Kamiela, Mariska, Freddy en Leen, bedankt voor alles! Het afgelopen jaar hebben we elkaar weer meer gezien, doordat veel van ons meer tijd hadden. Ik vind dat fijn en ben blij met al jullie steun.

# Contents

- Abstract..... 1
- Acknowledgements..... 2
- Contents..... 3
- 1. Introduction ..... 4
- 2. Materials & Methods..... 7
- 3. Results & Discussion ..... 11
  - 3.1 Removal location of major groundwater contaminants in rapid sand filters..... 11
  - 3.2 Mechanisms and capacity of manganese removal in the filter systems ..... 15
  - 3.3 The removal of ammonium in RSFs is biological and stratified..... 18
  - 3.3 Metagenomic analysis reveals guilds with different functionalities ..... 21
- 4. Conclusions ..... 25
- 5. Recommendations for further work ..... 26
- 6. References..... 27
- 7. Appendices..... 32
  - I. Protocol to prepare trace element solution..... 32
  - II. Physical characteristics of the filter bed material..... 33
  - III. Concentration profiles over dual bed..... 34

# 1. Introduction

## Rapid sand filters: the central element in drinking water production

In the Netherlands, 60-70% of all drinking water is produced from groundwater. Groundwater presents several advantages over the other common source, surface water, such as lower concentrations of contaminants and stable temperature and composition (Geudens & Grootveld, 2017). Nevertheless, treatment is still required to remove its main contaminants: iron, ammonium and manganese. Their presence causes organoleptic problems such as bad taste and odour as well as biological safety issues due to microbial regrowth (van Dijk et al., 2006).

Most of the drinking water treatment schemes rely on the use of chemical disinfectants to remove viruses and microorganisms and guarantee safe tap water. However, the resulting bad taste and potential enrichment of resistant bacteria make its use undesirable (Shi et al., 2013). In the Netherlands, water is treated using disinfectant-free systems based on biological processes. The most important operation in these processes is rapid sand filtration.

Rapid sand filters (RSFs) consist of a sand bed of approximately 2 meters in height. Water enters from the top and treated water leaves through the bottom (Figure 1-1). The sand bed behaves both as a reactor and a filter. Contaminants are oxidized by biological and/or physical-chemical reactions, which results in the formation of precipitates. Those precipitates are physically removed by the bed. The filtration step is preceded by an aeration step to oxygenate the water, which is required for the oxidation of contaminants. At the same time, undesired gasses like methane and hydrogen sulphide are stripped (Albers et al., 2015). In this way, high-quality drinking water can be produced without a chemical disinfection step.

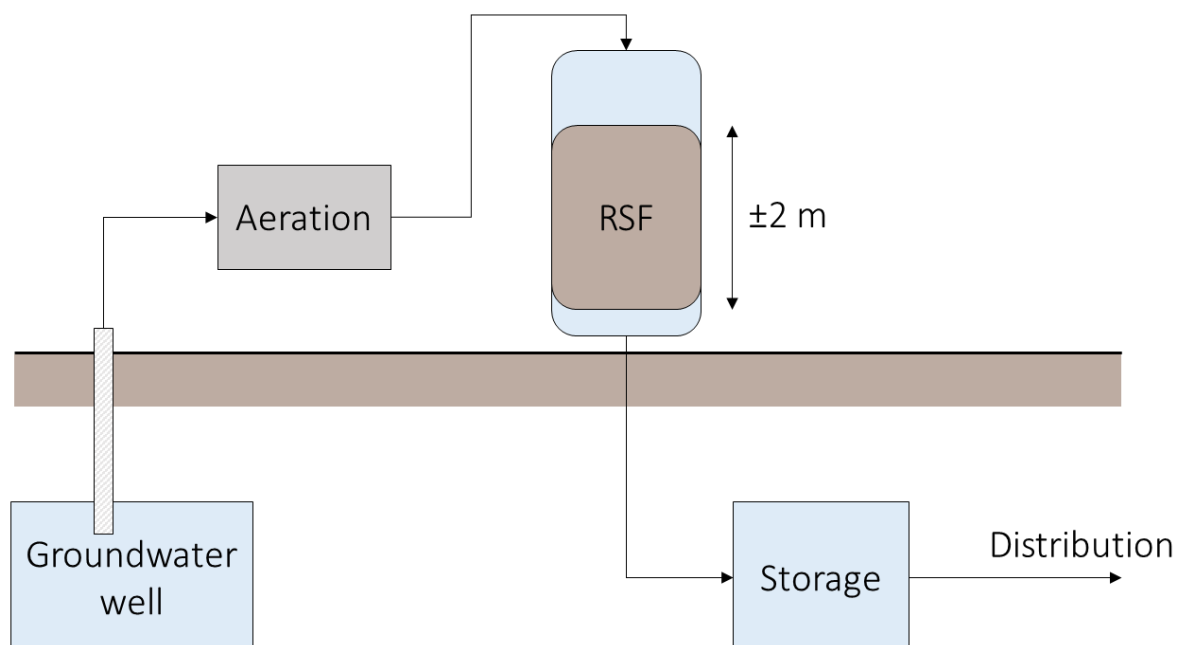
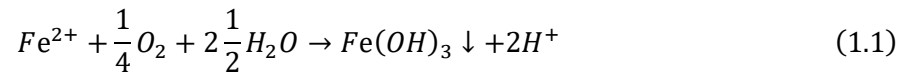


Figure 1-1. Schematic overview showing the different steps in the production of drinking water from groundwater. RSF = Rapid sand filter.

## Biological and chemical processes behind the removal of $Fe^{2+}$ , $NH_4^+$ and $Mn^{2+}$

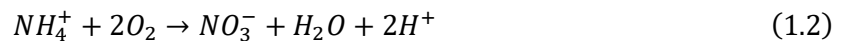
RSFs have been used for many years to produce drinking water, yet most of the removal mechanisms in the filter remain poorly understood. Over the years, a complex coating of oxides and microorganisms forms on the sand grains in the filter bed. This coating is responsible for the oxidation of the different contaminants.

Iron can be oxidized by three different processes. Soluble iron spontaneously oxidizes in the presence of oxygen, in a process known as homogenous iron oxidation (Equation 1.1) (Van Beek et al., 2012):



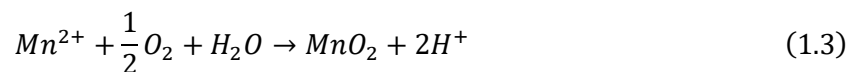
This reaction is an example, since other iron(hydr)oxides can form as well. The products of this reaction are insoluble iron(III)hydroxides which are removed by the bed (Sung & Morgan, 1980). The resulting oxides act as a catalyst in the heterogenous oxidation of iron, which results in more iron(III)hydroxides (Van Beek et al., 2012). Furthermore, iron oxidizing bacteria like *Gallionella* spp. & *Leptothrix* spp. have also been found to contribute to the removal of iron in RSFs (Katsoyiannis & Zouboulis, 2004; Van Beek et al., 2012).

Ammonium is oxidized to nitrate by nitrifying microorganisms. Equation 1.2 shows the overall oxidation reaction from ammonium to nitrate (Madigan et al., 2015):



The core taxa responsible for this reaction consist of the genera *Nitrosomonas* and *Nitrospira* (Albers et al., 2015; Gülay et al., 2016; Poghosyan et al., 2020). Besides, oxides present in the coating are also suggested to act as a catalyst in the chemical oxidation of ammonium (Guo et al., 2017).

Manganese can be oxidized heterogeneously or biologically. An example of the oxidation reaction of manganese is shown in equation 1.3 (Vries et al., 2017):



Heterogeneous oxidation is an autocatalytic reaction: the produced manganese oxides act as a catalyst in the same oxidation reaction (Davies & Morgan, 1989). Besides, biological removal of manganese can be performed by manganese oxidizing bacteria like *Leptotrix* spp., *Pseudomonas* spp. and *Bacillus* spp. (J. Bruins, 2017; Burger et al., 2008; Cerrato et al., 2010).

The different reactions occur at different heights in the filter. Increasing redox potentials are required for the oxidation of iron, ammonium and manganese, but the factors controlling the order are not fully understood (Mouchet, 1992). Not only the order is relevant, but also the interactions between the components. For instance, the nitrification process is inhibited by iron deposits and flocs and the removal of manganese only starts after complete oxidation of ammonium into nitrate (De Vet et al., 2009; Vandenabeele et al., 1995). All of these simultaneous interactions make the design of filters very challenging. So much, that sometimes different treatment schemes are required to treat water with a similar composition. This thesis focusses on the spatial distribution of genomic profiles and removal mechanisms in RSFs. To do so, two drinking water treatment plants which employ one and two RSFs to treat water with a similar composition were investigated.

The hypothesis of this thesis is that stratification of the removal processes takes place regardless of the plant configuration. Thus, different plant configurations yield similar profiles in the composition of the coating, removal mechanism and the microbial community, which explains the stratification of the removal processes.

### Research question

In this study, we chose two drinking water treatment plants treating groundwater with a similar composition using different plant operation systems: one dual bed filter and two single bed filters in series. This thesis focuses on the following question:

#### **How can genomic profiles and removal mechanisms explain the observed stratification of $\text{Fe}^{2+}$ , $\text{NH}_4^+$ and $\text{Mn}^{2+}$ removal in rapid sand filters?**

To answer this question, a combination of full- and lab-scale experiments, together with in-silico analysis were used. The composition of the coating on the grains and concentration profiles of contaminants in the plants were measured to find the locations in the filters responsible for the removal of each contaminant. Besides, batch tests were applied to quantify and distinguish between biological and chemical ammonium and manganese removal activities of filter bed samples from different heights. Furthermore, metagenomic analysis was performed to study the composition and functional potential of the community present on the sand grains.

# 2. Materials & Methods

## Sample collection

Filter material and water samples were collected from two Dutch drinking water treatment plants with a different configuration (Figure 2-1). One plant consists of two single bed filters in series, while the other plant consists of one dual bed filter. Filter operation parameters and raw water concentrations are shown in Table 2..

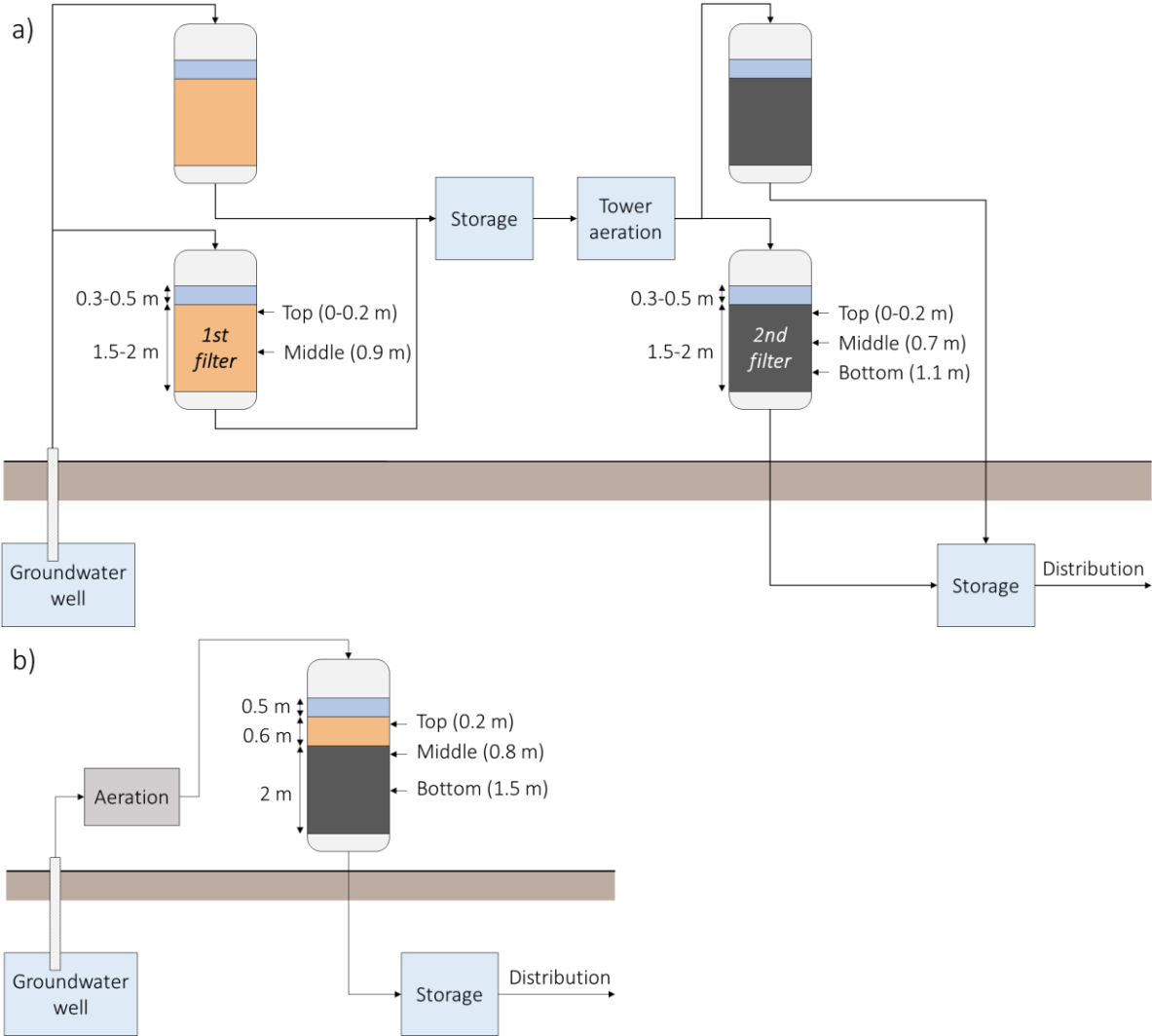


Figure 2-1. Schematic representation of the treatment schemes of both plants, with details on the locations where samples of the filter bed material were taken. The sampling depth is shown in meters from the top of the filter bed. The colours in the picture correspond to supernatant (blue) and the colours of the samples that were taken (orange and black). a) The sequential filter system with two single bed sand filters in series. The first filter has aeration on top of the filter. b) The dual bed filter consisting of an anthracite and a sand layer.

Water samples were taken of the raw groundwater and the effluent of each filter. Samples were collected along the height of the dual bed filter too. Triplicate water samples were taken in order to determine ammonium, nitrate, nitrite (N-species) and iron and manganese concentrations. All samples were immediately filtered through a 0.45 µm nanopore filter. Iron and manganese samples were acidified to pH<1 using 69% ultrapure HNO<sub>3</sub> to ensure all metals are dissolved. pH, O<sub>2</sub> concentration, temperature and redox potential were measured on-site using a multimeter (Multi 3630 IDS, Xylem Analytics, Germany). Sand samples were taken from each filter at different heights (Figure 2-1) using a peat-sampler.

Table 2.1. Operational parameters of both drinking water treatment plants and the raw water composition entering the filters. The historical data shows average concentrations together with the standard deviation for 7-8 measurements between November 2018 and July 2020.

	Unit	Dual bed	Sequential filters
<b>Filter height and media</b>		0.6 m anthracite 2.0 m sand	1.5-2 m sand
<b>Height of supernatant</b>	m	0.3-0.5	0.3-0.5
<b>Age of media</b>	years	1 (anthracite) 5 (sand)	< 3
<b>Filter area</b>	m <sup>2</sup>	28.3	15.2
<b>Filtration rate</b>	m/h	5.7	4.3
<i>On-site measurements</i>		<b>Raw water</b>	<b>Raw water</b>
<b>pH</b>		6.6	6.4
<b>T</b>	°C	12.1	11.5
<b>ORP</b>	mV	-104.2	-128.4
<b>O<sub>2</sub></b>	mg/L	0.024	0.025
<i>Historical data</i>			
<b>Fe<sup>2+</sup></b>	mg/L	6.5 ± 0.1	5.1 ± 0.2
<b>Mn<sup>2+</sup></b>	mg/L	0.67 ± 0.03	0.31 ± 0.02
<b>NH<sub>4</sub><sup>+</sup></b>	mg N/L	0.41 ± 0.02	1.9 ± 0.1
<b>NO<sub>2</sub><sup>-</sup></b>	mg N/L	< 0.003	< 0.003
<b>NO<sub>3</sub><sup>-</sup></b>	mg N/L	< 0.2	< 0.2

### Batch tests: maximum removal rates and adsorption/desorption experiments

The maximum removal rate of ammonium and manganese by the sand from the RSFs was determined in batch tests. 4 gram of wet sand, 200 mL of tap water and 100 µL of trace element solution (Appendix I) were mixed in 300 mL shake flasks. After an acclimatization period of 20-30 minutes at 25 °C and 150 rpm, each flask was spiked with 3 mL of 100 mg NH<sub>4</sub>-N/L NH<sub>4</sub>Cl or 100 mg Mn<sup>2+</sup>/L MnCl<sub>2</sub>·4H<sub>2</sub>O (SigmaAldrich, USA).

For the abiotic experiments, shake flasks were incubated overnight at 50°C with 0.05 g/L penicillin G sodium (SigmaAldrich, USA). Liquid was replaced the next morning and the batch test was performed as described before.

To study the desorption of manganese, a similar batch test was performed with a higher initial concentration. The experiment was performed using 190 mL of tap water and 10 mL of 100 mg Mn<sup>2+</sup>/L

MnCl<sub>2</sub>·4H<sub>2</sub>O. The next morning, liquid was replaced by fresh water without manganese and the desorption was followed.

Samples of 1 ml were taken at different time intervals throughout the entire process. Manganese samples were immediately filtered through a 0.2 µm nanopore filter. Adsorption and desorption samples were diluted with MilliQ water and acidified with 69% HNO<sub>3</sub>. Samples were stored in the fridge until further analysis.

### Analytical procedures

The ammonia, nitrate and nitrite concentration were determined the same day using photometric analysis (Gallery Discrete Analyzer, Thermo Fisher Scientific, USA) and samples were stored -20°C afterwards. Metal samples were analysed by ICP-MS. Unfiltered metal samples were filtered after at least 16 hours of acidification for total metal quantification.

For the detection of ATP, 1 mL of water was added to 1 g of sand. The samples were sonicated for 1 min at an output power of 15 W and a frequency of 20 kHz (ultrasonic homogenizer, Qsonica sonicators, USA). Samples were subsequently filtered through a 0.22 µm pore-size filter. The concentration of ATP in the liquid was determined in duplicates using an ATP analyser as described by the manufacturer (Clean-Trace™ Luminometer NG3, 3M, USA).

### Characterisation of the filter bed material

To check the composition of the coating, 1.5 gram of wet sand was frozen overnight at -80 °C and freeze-dried during 48 h (Alpha 1-4 LD plus, Christ, Germany). The coating was extracted in triplicate using 40 mL citrate buffered dithionite (CBD) solution (Claff et al., 2010). After 4 hours, samples were centrifuged at 4000 rpm for 10 minutes and filtered through a 0.45 µm filter. Iron was measured using the 3500-Fe B. Phenanthroline Method (3500-Fe IRON, n.d.). Manganese was measured using colorimetric measurement (LCK, Hach Lange, The Netherlands). Besides, the dual bed middle and bottom sample were manually separated into an anthracite and sand fraction to study the penetration on anthracite into the sand layer. Extraction of the coating was performed once on these fractions. The concentration of iron was measured using ICP-OES.

### DNA extraction

The extraction of nucleic acids was done using bead beater tubes from the MagMAX CORE Mechanical Lysis Module and the solutions from the MagMAX CORE Nucleic Acid Purification Kit (Applied Biosystems, Thermo Fisher Scientific, USA). This combination was used to improve the DNA recovery. The following steps were done twice for each sample: 0.25 g of sample, 350 µL lysis solution and 10 µL proteinase K were mixed in bead beater tube. Samples were beaten for 2x30 seconds (Bead Mill Homogenizer, BioSpec, USA) and centrifuged for 2-7 minutes at 10000 g until supernatant was clear. Supernatants of two tubes were combined in a clean tube, mixed with 450 µL and 20 µL Bead/PK mix and vortexed for 10 min at maximum speed. The tubes were placed on a magnetic stand for 1 min and the supernatant was removed. The samples were washed twice by adding 500 µL of wash solution 1/2 and vortexing for 1 minute. The supernatant was removed after 1 minute on the magnetic stand. After the second washing step, samples were air-dried for 5 minutes. 90 µL elution buffer was added and samples were vortexed for 10 min. After 2 min on the magnetic stand, the supernatants were transferred to clean tubes. All samples except dual bed top and bottom were purified afterwards using the GeneJET PCR Purification kit following the protocol supplied by the manufacturer (Thermo Scientific, Thermo Fisher Scientific, USA). DNA was quantified as prescribed by the manufacturer using the Qubit 4 Fluorometer and Qubit dsDNA HS assay kit (Invitrogen, Thermo Fisher Scientific, USA).

### Sequencing procedure

Library preparation of the metagenomes was done using the Nextera XT kit (Illumina, San Diego, California U.S.A.) according to the manufacturer's instructions. Enzymatic tagging was performed starting with 1 ng of DNA, followed by incorporation of the indexed adapters and amplification of the library. After purification of the amplified library using AMPure XP beads (Beckman Coulter, Indianapolis, USA), libraries were checked for quality and size distribution using the Agilent 2100 Bioanalyzer and the High sensitivity DNA kit (Agilent, San Diego, USA). Quantitation of the library was performed by Qubit using the Qubit dsDNA HS Assay Kit (Invitrogen, Thermo Fisher Scientific, USA). The libraries were pooled, denatured and sequenced with the Illumina MiSeq sequence machine (San Diego, California USA). Paired end sequencing of 2 x 300 base pairs was done using the MiSeq Reagent Kit v3 (San Diego, California USA) according to the manufacturer's instructions.

### Metagenomic pipeline

Raw sequencing data was quality-filtered and trimmed using Trimmomatic v0.39 (HEADCROP:16 LEADING:3 TRAILING:5 SLIDINGWINDOW:4:10 CROP:240 MINLEN:35) (Bolger et al., 2014). Data was analysed using FastQC v0.11.7 before and after trimming (Andrews, 2010). MEGAHIT v1.2.9 was used to assemble the trimmed reads into contigs (D. Li et al., 2015). The raw reads were mapped back to the contigs using BWA-MEM2 (Md et al., 2019). SAMtools was used to determine statistics of the contigs and evaluate the mapping (H. Li et al., 2009). Taxonomic annotation of the contigs was performed using the Contig Annotation Tool (CAT) (von Meijenfeldt et al., 2019). The results of the taxonomic annotation and the mapping were combined to obtain the relative abundances for all taxa. RStudio v1.4.1106 was used for the data analysis and production of the plots (RStudio Team, 2021).

### 3. Results & Discussion

#### 3.1 Removal location of major groundwater contaminants in rapid sand filters

The coating on the grains from the first and second section mainly consists of Fe and Mn respectively

Manganese and iron precipitate in the form of oxides, which permanently remain in the filter on the sand grains (Davies & Morgan, 1989; Van Beek et al., 2012). Thus, as shown by previous studies, the composition of the coating reflects the removal location of each contaminant during the lifespan of the filter (Gude et al., 2016; Gülay et al., 2014). In order to study the coating composition, the amount of iron and manganese was determined for all the filter bed samples after extraction using citrate buffered dithionite (Figure 3-1) (Claff et al., 2010).

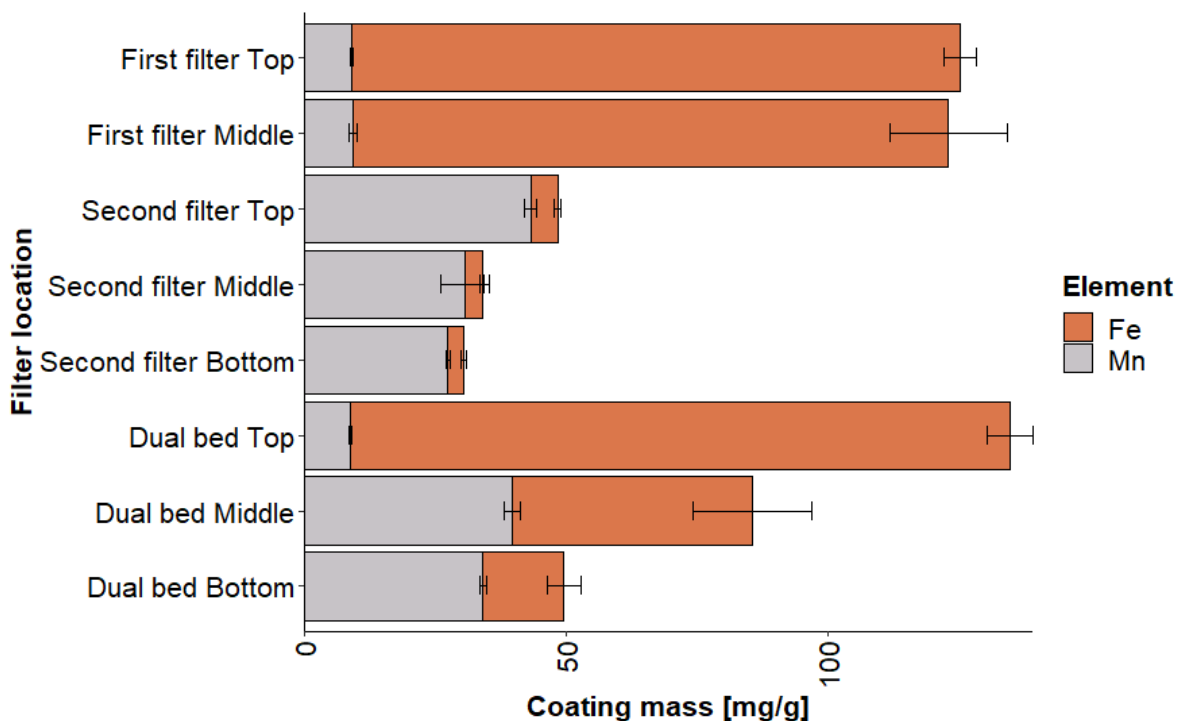


Figure 3-1. Average coating composition together with the standard deviation for all the filter bed samples. The mass of Fe (orange) and Mn (grey) in the coating is shown in  $\text{mg/g}_{\text{bed}}$ . Triplicate measurements were performed.

The coating of the samples from the first sections, i.e. dual bed top and first filter, mainly consisted of iron ( $118 \pm 8 \text{ mg}_{\text{Fe}}/\text{g}_{\text{sand}}$ ). Similarly, the coating of the sand from the second sections, i.e. dual bed middle/bottom and second filter, mainly consisted of manganese ( $33 \pm 6 \text{ mg}_{\text{Mn}}/\text{g}_{\text{sand}}$ ), within the range of 0.58 and 69 mg/g observed before (Breda et al., 2019). The composition of the coating shows iron is mainly removed in the first part of the filter and manganese in the second part. Concentration profiles of the water over the filter height were measured to verify the removal locations

Interestingly, the amount of manganese on the coating of sand from different filters is similar. Based on the higher influent concentration (0.6 and 0.3  $\text{mg Mn}^{2+}/\text{L}$ ) and older filter bed (5 and <3 years) of the dual bed, higher amounts of manganese were to be expected in this sand layer. However, the backwash

program is very intense in both cases: upward water velocities of 40 m/h for the dual bed and 10 m/h in combination with air for the sequential filters. Predicting the composition of the coating based on process parameters is still challenging, showing that more research is necessary to better understand the processes happening in the filters.

### Anthracite penetration into the sand layer results in iron presence in the second part of the dual bed

The coating of dual bed middle and bottom samples contains a significant amount of iron, while the samples of the second filter barely contain any (Figure 3-1). The presence of iron in the coating of the samples originating from the second layer of a dual bed was also observed previously (Gude et al., 2016). We hypothesize that penetration of anthracite grains into the sand layer might explain the presence of iron in these samples.

To study this hypothesis, the grains from dual bed middle and bottom were manually separated in an anthracite and sand fraction based on size and shape. Weighing the individual fractions showed 25% of the middle sample and 6% of the bottom sample consisted of anthracite. The composition of the coating of these fractions was determined as well. This resulted in higher amounts of iron per gram of anthracite ( $190 \pm 20 \text{ mg}_{\text{Fe}}/\text{g}_{\text{sand}}$ ) compared to the amount determined for anthracite from dual bed top ( $126 \pm 4 \text{ mg}_{\text{Fe}}/\text{g}_{\text{sand}}$ ), but the values are in the same order of magnitude. The coating of the anthracite fraction mainly contained iron, while manganese is the main component of the coating in the sand fraction (Figure 3-2). In conclusion, these results confirm that the presence of iron in the coating of dual bed middle and bottom (Figure 3-1) is caused by the penetration of anthracite into the sand layer. This penetration might influence the performance of the middle and bottom filter layers. The catalytic surface area per volume of bed for manganese oxidation decreases, likely hampering manganese removal. Besides, nitrification is known to be inhibited by the presence of iron (De Vet et al., 2009).

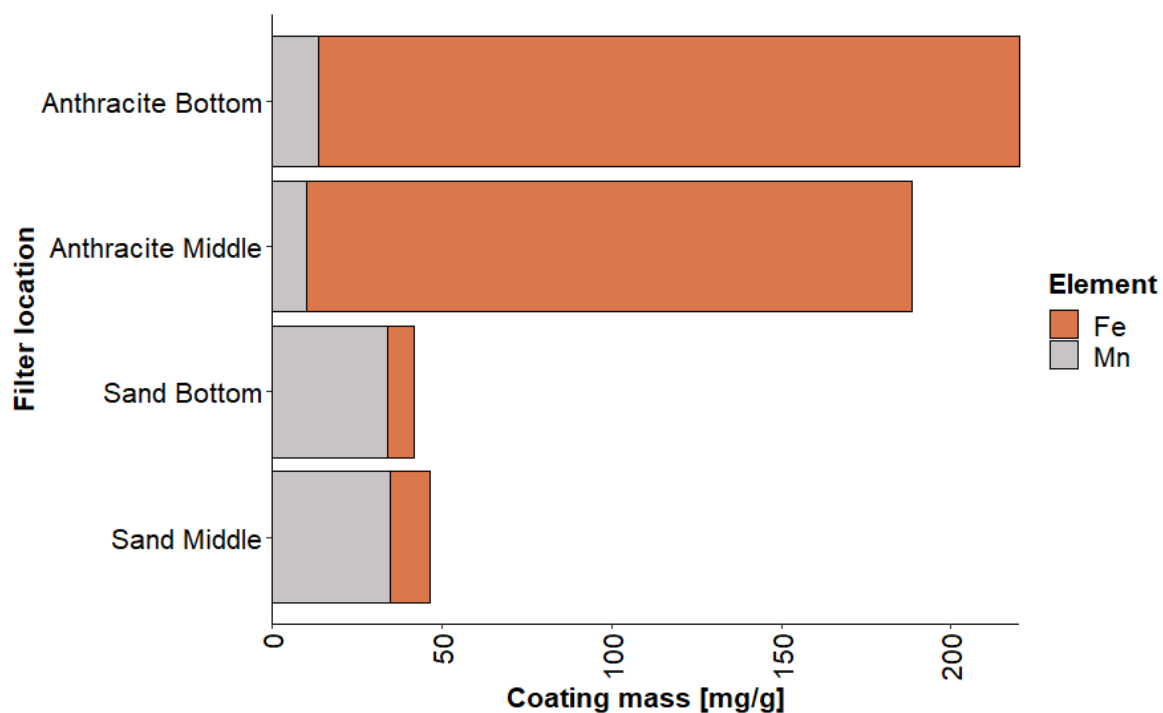


Figure 3-2. Coating composition of the anthracite and sand fractions from dual bed middle and bottom samples. The mass of Fe (orange) and Mn (grey) in the coating is shown in  $\text{mg}/\text{g}_{\text{bed}}$ .

## **The removal of Fe<sup>2+</sup> and Mn<sup>2+</sup> takes place in separate filter sections and NH<sub>4</sub><sup>+</sup> is removed in parallel with both**

Influent and effluent water samples of each section were analysed to study the removal location of the major groundwater contaminants (Figure 3-3a, b). In both the dual bed and the sequential filter system, iron is the first component to be removed, and removal takes place at the equivalent location – first section - in the treatment scheme. The removal of manganese mainly (> 93%) takes place in the subsequent parts of treatment scheme - in the sand layer of the dual bed and the 2<sup>nd</sup> filter. These results are in line with the removal location reflected by the composition of the coating.

Ammonium removal is observed in both sections, together with the removal of iron in the first section and manganese in the second section. Most NH<sub>4</sub><sup>+</sup> removal (> 71%) takes place in the second section of both plants. The simultaneous removal of iron and ammonium has been observed before (Gude et al., 2016; Lee et al., 2014). However, several studies also reported an inhibiting effect of iron on nitrification (De Vet et al., 2009; Gouzinis et al., 1998). We hereby report that nitrifying organisms can be present and active in the presence of iron. However, the age of the filters could be the underlying reason. De Vet et al. (2009) observed co-occurrence of iron removal and nitrification in young filters, but nitrification capacity decreased when the filter matured. The decrease in nitrification capacity correlated with an increase in the amount of iron deposits on the sand grains. The anthracite layer and first filter are both fresh (< 3 years old), thus we believe the age of the filter explains the co-removal of ammonium and iron. To further understand this phenomenon, metagenomic analysis was performed to study the microbial community responsible for the removal of contaminants.

During the start-up of filter, the conversion of ammonium into nitrate has to be complete before manganese removal starts (Tekerekopoulou et al., 2013). Suggested reasons are the necessary development of the redox potential or the inhibition of biological manganese oxidation by nitrite (Mouchet, 1992; Vandenaabeele et al., 1995). However, in both filter systems the removal of manganese and ammonium takes place simultaneously instead of sequentially. Simultaneous removal has been observed for mature filter receiving water with an ammonium concentration below 2 mg/L (Gouzinis et al., 1998; Gude et al., 2016).

The two-step oxidation of ammonium to nitrite and nitrate was also followed (Figure 3-3c, d). The full conversion into nitrate is complete after the second section. The historical data also show complete conversion of ammonium into nitrate (Table ), and nitrogen balances close in both locations. Nitrite was not detected in any location, so it does not accumulate in the filter system.

The concentration profiles over the filter demonstrate the removal location of the main contaminants. Iron is removed in the first section, manganese in the second section and ammonium removal is ubiquitous. The removal locations suggests a spatial division in the distribution of microbial guilds able to oxidize the different contaminant.

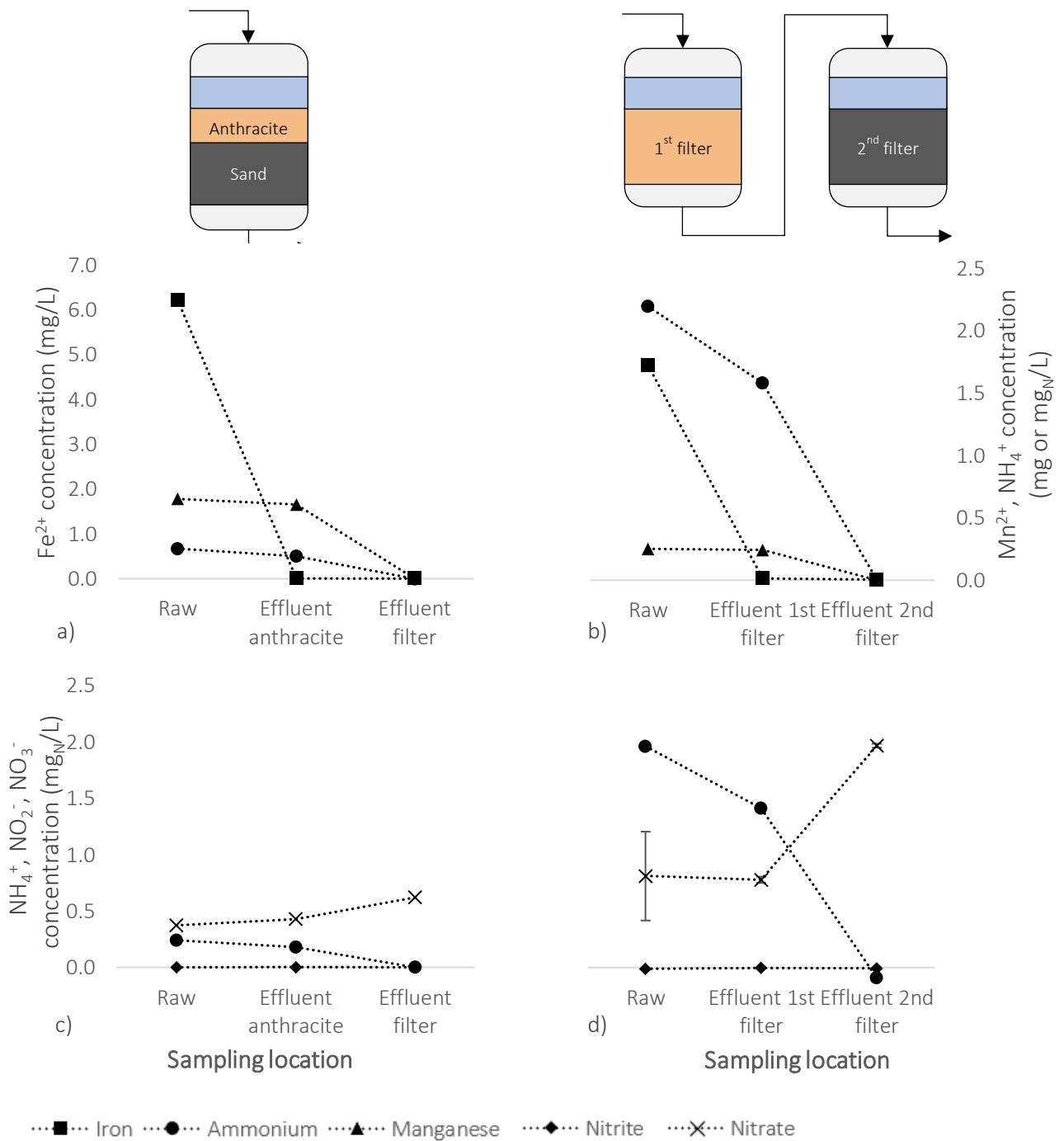


Figure 3-3. Concentrations in the raw water and effluent of both section for the dual bed (a, c) and the sequential filter system (b, d). On the top, a schematic overview of the plant configurations is shown. The colours of the sections correspond to the main component of the coating: Mn (grey) or Fe (orange). The concentrations of nitrogen compounds are shown in mg N/L. Averages and standard deviation resulting from duplicate measurements are shown for the nitrogen species of the sequential filter system (d).

Table 3.1. Historical data showing average concentrations (mg N/L) and the nitrogen balance of both drinking water treatment plants based on at least 4 measurements between 2018 and 2020.

	Raw water concentrations			Plant effluent concentrations			N-balance
	NH <sub>4</sub> <sup>+</sup>	NO <sub>2</sub> <sup>-</sup>	NO <sub>3</sub> <sup>-</sup>	NH <sub>4</sub> <sup>+</sup>	NO <sub>2</sub> <sup>-</sup>	NO <sub>3</sub> <sup>-</sup>	
Dual bed	0.41	<0,003	<0,2	<0,02	<0,003	0.37	0.91
Sequential filters	1.77	<0,003	<0,2	<0,03	<0,01	1.81	1.02

### 3.2 Mechanisms and capacity of manganese removal in the filter systems

#### The two filter sections show different manganese removal mechanisms: adsorption and oxidation

Manganese removal mainly takes place in the second section of the filter systems (Figure 3-3) and is the major component in the coating on the sand of this section (Figure 3-1). Not only the removal location is of interest, but also the removal mechanism. To understand how manganese is being removed in the filters, the mechanisms and catalytic capacity of manganese removal were followed in batch tests. Filter bed material from the second sections removed all manganese (Figure 3-4a, grey points), while removal by the sand from the first sections did not, and an equilibrium was reached (Figure 3-4a, orange points). This difference indicates that different removal mechanisms occur in the first and second filter section. Manganese oxides present in the coating of the samples from the second section (Figure 3-1) catalyse the oxidation of manganese, while iron(hydr)oxides present in the coating of the samples from the first section (Figure 3-1) can adsorb manganese (Davies & Morgan, 1989).

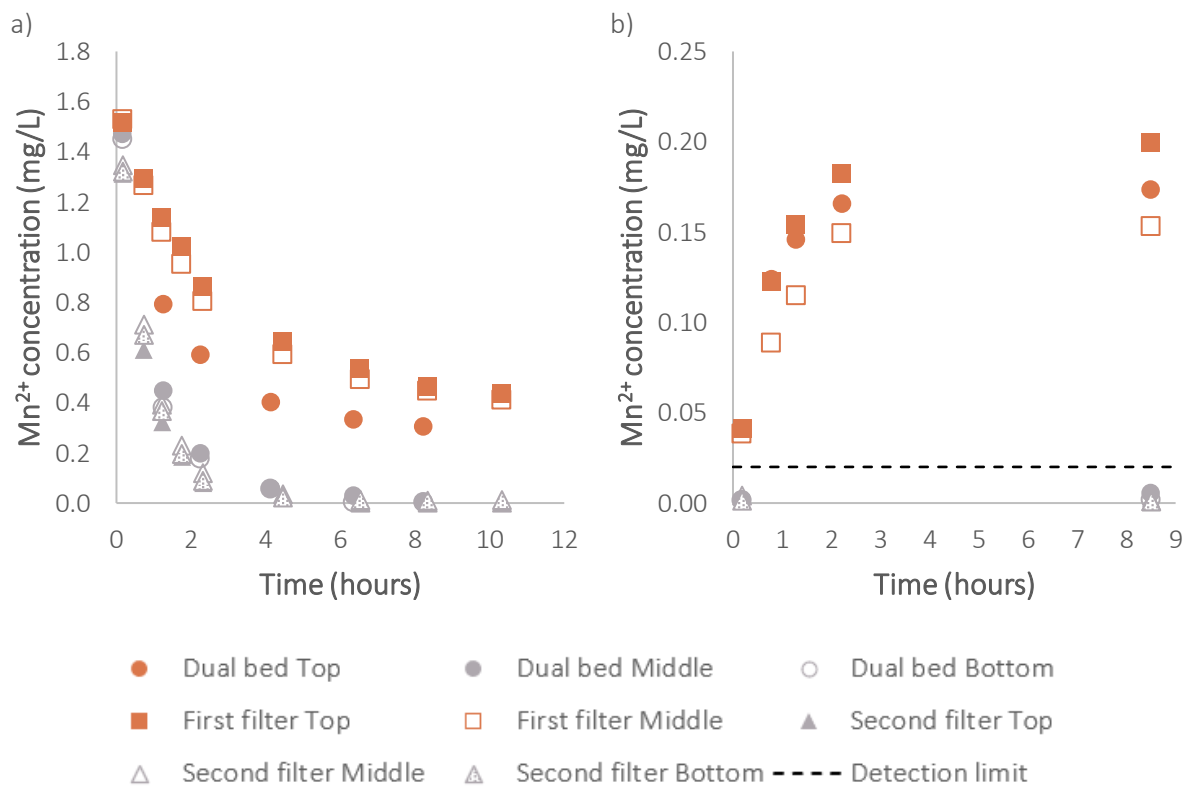


Figure 3-4. Removal (a) and desorption (b) of Mn<sup>2+</sup> in a batch test with filter bed material from all filters. The colour of the points corresponds to the main component of the coating: Mn (grey) or Fe (orange).

To investigate the different mechanisms, manganese desorption was followed for all samples. Desorption was only observed for the samples from the first filter sections (Figure 3-4b), which indicates that these filter layers remove manganese through adsorption rather than oxidation. On the other hand, filter bed material from the second filter sections did not show any desorption (Figure 3-4b), meaning these samples catalyse the oxidation of manganese. The adsorption capacity of sand in the top layer of the filter was predicted by a model for the removal of manganese and iron in RSFs, but only under

anaerobic conditions (Vries et al., 2017). Buamah et al. (2008) observed removal of manganese until an equilibrium by iron-oxide coated sand from a first filter under both oxic and anoxic conditions. To our knowledge, this is the first study that used adsorption and desorption experiments to show the different mechanisms responsible for  $Mn^{2+}$  removal. Further research is required to quantify the relevance of these mechanisms for the overall manganese removal in full-scale rapid sand filters. The removal of manganese occurs in the second section of the filter (Figure 3-3), so the oxidation of manganese likely is the most important mechanism in the full-scale process and further analysis therefore focussed on this removal mechanism.

### **Manganese oxidation capacity remains constant over the filter height**

The oxidation of manganese by manganese oxides is known to be a first-order reaction. The first order rate constants can thus be determined to quantitatively compare the manganese removal capacities of the different filter samples. The first order rate constant ( $k$ ), concentration of manganese ( $[Mn^{2+}]$ ) and reaction time ( $t$ ) are related in the following way (Katsoyiannis & Zouboulis, 2004):

$$\ln[Mn^{2+}]_t = \ln[Mn^{2+}]_0 - kt \quad (3.1)$$

To determine the rate constants for the removal of manganese, the results of the batch tests (Figure 3-4a) were fitted to equation 3.1. The observed rate constants are in the range of 0.01 to 0.017  $\text{min}^{-1}$  (Figure 3-5). This is higher than the rate constants of 0.004-0.005  $\text{min}^{-1}$  observed under similar conditions in the only study where manganese removal by sand from an RSF was studied in a batch test (Sahabi et al., 2009). The larger amount of sand used in this study, 2 g of sand per 100 mL of water instead of 0.5 g in 100 mL used by Sahabi et al. (2009) explains the difference in observed rate constants. A standard method to measure the rate constants is required to compare studies among each other, and more studies are needed to quantitatively understand the role of each manganese removal mechanisms in RSFs.

The rate constants observed for the second filter and dual bed bottom are in the same range ( $0.0015 \pm 0.001$  and  $0.0013 \pm 0.002 \text{ min}^{-1}$ ) (Figure 3-5). Those results are in accordance with the composition of the coating, which show similar amounts of manganese for these samples (Figure 3-1). Breda et al. (2019) showed that manganese capacity depends on available surface area of manganese oxides, rather than the amount of manganese in the coating. The external surface area of the sand grains was determined using the Brunauer–Emmett–Teller theory (Brunauer et al., 1938). In accordance, the external surface area was indeed comparable for our samples ( $2.7\text{-}3.3 \text{ m}^2/\text{g}$ ) (Appendix II).

Manganese reaches until both dual bed middle and bottom in the filter (Appendix III), so manganese removal capacity was expected for both samples. The rate constant of dual bed middle is lower than observed for dual bed bottom (Figure 3-5). We hypothesize that anthracite penetration is the underlying reason for this observation. The dual bed middle sample consists for 25% of anthracite, but the iron(hydr)oxides on the anthracite (Figure 3-1) do not oxidize manganese (Figure 3-4). Correction of the rate constant of dual bed middle using this anthracite ratio results in a value of  $0.0014 \pm 0.002 \text{ min}^{-1}$ , which is comparable to the other rate constants. To conclude, manganese oxidation capacity of the sand remains constant over the height of both filters, but the observed removal capacity of the dual bed middle sample is lower due to anthracite penetration. The constant removal capacity over the height of the filter could be a result of mixing due to backwashing.

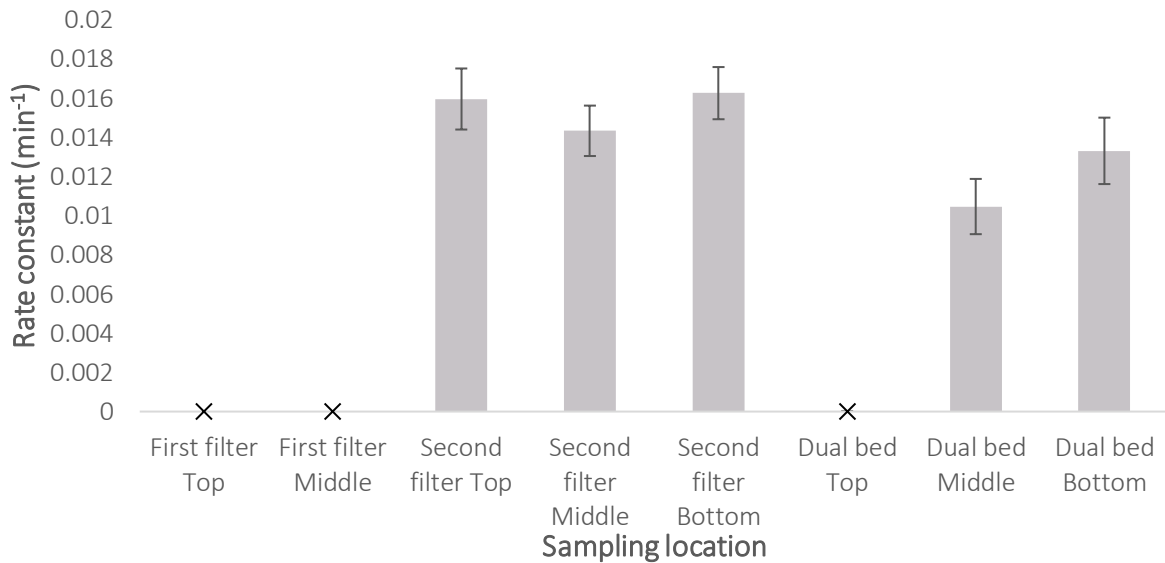


Figure 3-5. First order rate constants of Mn<sup>2+</sup> oxidation by filter bed material in batch. The average rate constant and standard deviation of duplicate measurements are shown and samples where manganese was not oxidised (x) are excluded.

### The effect of anthracite penetration on the rate constants of manganese oxidation is also visible in the filter

The rate constants of manganese oxidation in the filter were determined to study the effect of anthracite penetration within the filter as well. To determine the rate constant of manganese oxidation in the filter, the reaction time in equation 3.1 was substituted by empty bed contact time (EBCT) (Katsoyiannis & Zouboulis, 2004):

$$EBCT = \frac{\text{Column height (m)}}{\text{Flow velocity } (\frac{m}{h})} \times 60 (\frac{min}{h}) \quad (3.2)$$

The rate constants of manganese oxidation could be determined for two parts of the filter bed: 105-155 cm and 155-205 cm from the top of the supernatant (Appendix III), corresponding to the sampling location of the middle and bottom sample. In the dual bed filter, k-values of 0.47 and 0.57 min<sup>-1</sup> were observed at the height of the middle and bottom sample respectively. Those values are within the range of 0.14-0.69 min<sup>-1</sup> observed in column experiments and full-scale filters (Cai et al., 2015; Cheng et al., 2017; Katsoyiannis & Zouboulis, 2004). To sum up, this finding supports the conclusions drawn in the previous sections, where it seems that the bottom section of the filter bed has a higher rate constant than the middle one due to the penetration of anthracite into the sand layer.

### 3.3 The removal of ammonium in RSFs is biological and stratified

#### Biological processes are responsible for the removal of ammonium in RSFs

Although nitrifying bacteria have been extensively found in RSFs, chemical ammonium oxidation has also been suggested to play a role in the filters (Albers et al., 2015; Gülay et al., 2016; Guo et al., 2017). To study whether ammonia removal in the filters is of biological or chemical origin, batch activity tests were performed. The addition of penicillin G and overnight incubation at 50°C was used to differentiate between total and chemical ammonia removal. The amount of ATP on the filter bed material was measured before and after the penicillin treatment to evaluate the efficiency in suppressing the microbes (Pharand et al., 2014). Microbial activity was only detected on untreated filter bed material (Figure 3-6a), which indicates the used method was sufficiently efficient in killing the microbes. The amount of ATP detected on the sand is much lower than the  $10^2$  to  $10^3$  ng/cm<sup>3</sup> observed as average by Pharand et al. (2014). However, they also reported values as low as observed in this study, which shows the variability is large. After the treatment with penicillin, the filter bed material did not show any ammonium removal capacity (Figure 3-6b). Contrarily, a decrease in nitrification capacity has also been reported after microbial inactivation (Olańczuk-Neyman et al., 2000). However, this study only inactivated for 30 min at 50°C, which could be insufficient to kill all the microorganisms.

To conclude, to the best of our knowledge, we show for the very first time that ammonium removal in rapid sand filters is exclusively of biological origin. Moreover, we propose that the loss of ammonium removal capacity can be used in future studies as a proxy of microbial activity, i.e. to verify the efficiency of microbial inactivation methods. Currently, most-probable number technique is used to verify the killing efficiency of different methods (Yang et al., 2020). However, this technique greatly underestimates the number of active bacteria in soils and sediments (Belser & Mays, 1982). The use of a more reliable method, such as loss of ammonium removal capacity, can greatly benefit the study of the contribution of biological reactions to the removal of other groundwater contaminants such as manganese.

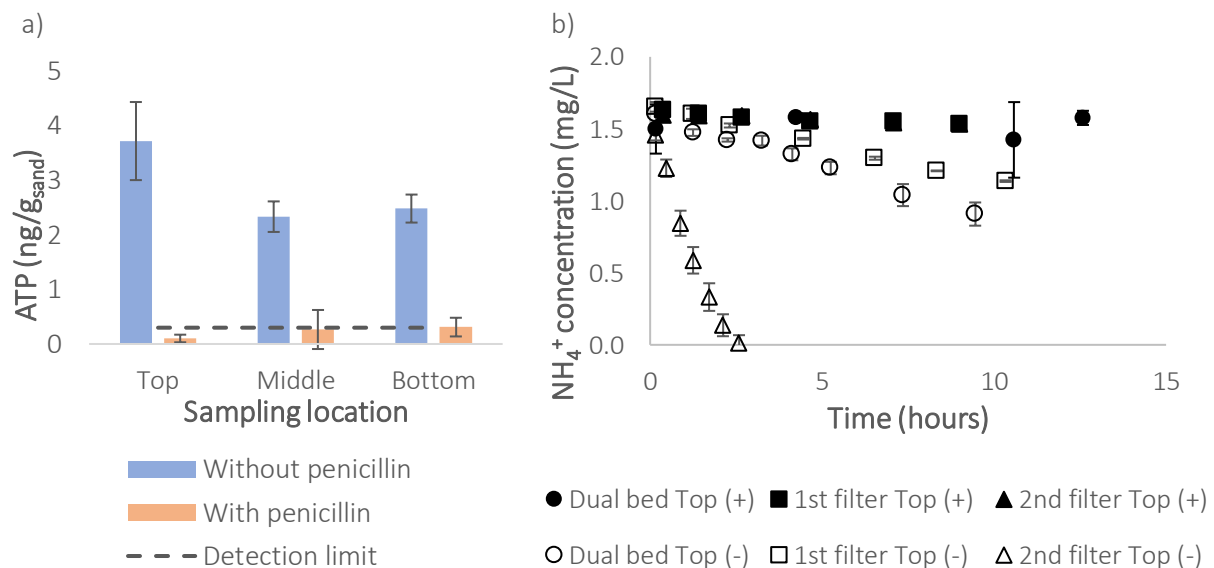


Figure 3-6. Amount of ATP present on the filter material from the dual bed filter before and after treatment with penicillin (a) and the removal of ammonium by the three samples before (-) and after (+) penicillin treatment (b). The three top samples are representative for the other samples which are not shown. The standard deviations of duplicate measurements are also shown in both graphs.

### Maximum ammonium removal rates show stratified removal of ammonium

Concentration profiles of the three full-scale filters showed that ammonium removal takes place in all filter sections. To compare the ammonium removal capacities of the different sand samples, maximum removal rates were determined in batch tests. Sand from the second section of both plants exhibit the highest rates (Figure 3-7), which corresponds to the filter location where most ammonium is removed (Figure 3-3). The sequential filter system shows higher removal rates than the dual bed filter, probably due to the higher ammonia influent concentration (Figure 3-3).

Previous studies showed higher removal rates at the top compared to the bottom of pilot- and full-scale filters due to the ammonium concentration gradient over the filter (Lee et al., 2014; K. Tatari et al., 2016; van den Akker et al., 2008). A similar stratification was visible in the maximum removal rates of the second filter, but not for the dual bed, where the maximum removal rates are the same. To see the effect of anthracite penetration, the rates were normalised per volume of sand using the sand-to-anthracite ratio determined before. Stratification in the second section of the dual bed became visible after this normalisation as well (blue bars, Figure 3-7). A similar profile, with lowest removal on top and highest removal in the middle was also seen in filters where subsurface aeration was applied to remove part of the iron before water enters the filter (de Vet, Dinkla, et al., 2011).

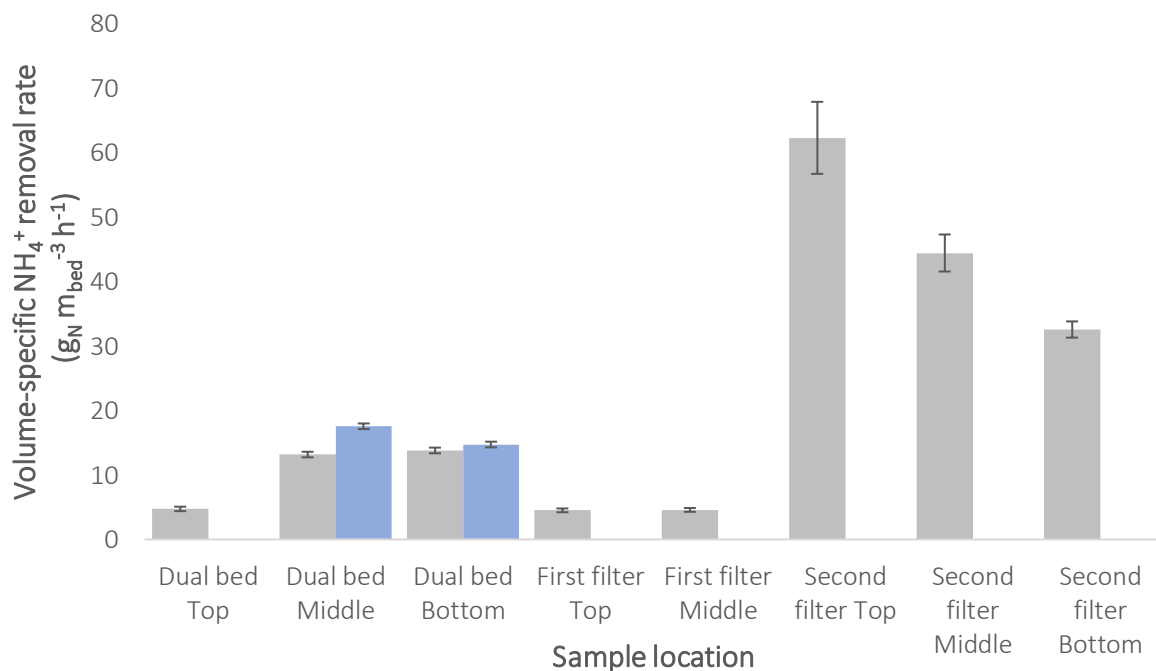


Figure 3-7. Maximum ammonium removal rates of the RSF samples including the standard deviations. Blue bars: rates of dual bed middle and bottom normalised per volume of sand using the sand/anthracite ratio of those samples.

Surprisingly, sand grains from dual bed bottom showed nitrification activity in batch tests, even though all ammonium is already removed before this location in the filter (Appendix III). We hypothesize this could be due to backwashing, and propose two different explanations. Intense backwashing might result in mixing of the sand grains (Schoonenberg, n.d.). In this case, their movement may result in exposure to alternating concentrations of ammonium, in a feast/famine-like regime. As a result, nitrifying guilds would be present at all filter heights. Alternatively, the removal of active nitrifiers during backwashing (de Vet, Kleerebezem, et al., 2011) could result in lower overall removal rates and deeper penetration of ammonium into the bed.

The effect of mixing due to backwashing is expected to cause a similar effect for both manganese and ammonium removal processes. However, our findings show that that ammonium removal is stratified, while manganese oxidation is not. We propose two different hypothesis to explain this behaviour. First, ammonium is biologically removed and microorganisms can quickly respond to an abundance or lack of substrates, resulting in an increase or decrease in observed activity. The activity could be more equally distributed just after backwashing, but others also observed a stratification immediately after backwashing (Lee et al., 2014). Secondly, the number of available catalytic sites for manganese oxidation does barely increase once the entire grain is covered, resulting in a constant catalytic capacity over the filter bed.

In conclusion, the removal capacity of ammonium is stratified for both filter systems, while the removal capacity of manganese remains constant over the height of the filter. It is suggested that the available area of manganese oxides remains rather constant and therefore the catalytic capacity of manganese removal as well. On the other side, microorganisms are stratified as a response to the concentration gradient of ammonium over the filter. More research is required to better understand this difference in stratification behaviour and the implications in the full-scale filters. Activity test should be performed with sand coated with different amounts of manganese and different available surface areas to see the effect on the removal capacities.

#### **Ammonium removal rates observed in the filter are lower compared to the rates observed in batch**

To study the removal of ammonium in the filter, removal rates of two sections of the dual bed were compared. The ammonium removal rates within the dual bed filter were determined using the concentration difference between two filter bed heights: 55-105 and 105-155 cm, which correspond to the top and middle samples. The results show volumetric removal rates of  $1.1 \text{ g m}_{\text{bed}}^{-3} \text{ h}^{-1}$  and  $2.6 \text{ g m}_{\text{bed}}^{-3} \text{ h}^{-1}$  respectively. This is within the range of removal rates observed by Lee et al. (2014) in column based experiments.

The rates observed in the filter are one order of magnitude lower than the rates observed in the batch test. The difference in temperature between the two systems could be an explanation: reaction rates are generally higher with increasing temperature and microorganisms become faster at higher temperatures. Another option is the availability of surface area. In the batch test, the total surface of the sand is available, while the available area is more limited in a packed bed. On the other hand, phosphate limitation might have lowered the observed rates. The phosphate concentration was  $26 \pm 7$  and  $9 \pm 6 \text{ } \mu\text{g P/L}$  during the batch tests and in the sand layer of the dual bed respectively. A linear relationship between the availability of phosphate and nitrification rate was reported for concentrations between 10 and 50  $\mu\text{g P/L}$  (De Vet et al., 2012). This means nitrification could be more limited by phosphate availability in the filter compared to the batch, explaining the lower rates observed in the filter.

To conclude, the rates observed in the filter are lower than observed in the batch test. These results highlight the importance of process operation conditions on the performance of rapid sand filters, and set the groundwork for possible optimization strategies.

### 3.4 Metagenomic analysis reveals guilds with different functionalities

#### Statistics of sequencing and assembly

The microbial community present on the sand plays an important role in the removal of contaminants. It is the only responsible for the removal of ammonium (Figure 3-6), and might also play a role in removing manganese and iron. To study the microorganisms present in the community, a metagenomic analysis was performed. DNA extracted from all sand samples was sequenced resulting in 1-10 million paired-end reads per sample (Table 3.). Trimmed reads were assembled *de novo* into contigs. Filtering out short contigs (<500 bp) resulted in 14-170 thousand contigs with an average size of 841-1273 bp. 44-89% of the raw reads could be mapped back to the contigs. Taxonomic analysis was performed on the contigs using a tool specifically designed to annotate contigs.

Table 3.2. Characteristics and statistics of the reads and filtered contigs (>500 bp) from all RSF samples.

	Dual bed			First filter		Second filter		
	Top	Middle	Bottom	Top	Middle	Top	Middle	Bottom
Raw reads	6.24E+06	2.93E+06	1.37E+06	8.42E+06	8.27E+06	1.04E+07	8.83E+06	9.68E+06
Trimmed reads	6.22E+06	2.82E+06	1.32E+06	8.40E+06	8.24E+06	8.40E+06	8.77E+06	4.93E+06
Contigs	4.27E+04	3.68E+04	1.38E+04	1.45E+05	1.46E+05	1.68E+05	1.61E+05	1.01E+05
Average size	1273	967	841	1187	1200	1075	1041	990
N50	1444	953	783	1323	1353	1074	1036	981
Total bp in contigs	5.44E+07	3.56E+07	1.16E+07	1.73E+08	1.75E+08	1.80E+08	1.67E+08	1.00E+08
Longest contig	1.07E+05	9.13E+04	1.09E+05	1.32E+05	1.44E+05	1.57E+05	9.20E+04	6.76E+04
% reads mapped to contigs	88.80%	54.60%	43.70%	83.60%	83.80%	79.90%	77.60%	67.70%

The percentage of reads that could be mapped back to the contigs is very low for the middle and bottom sample from the dual bed (Table 3.), so many reads did not end up in the contigs. The sequencing depth might have been too low to cover the diversity of the library. Therefore, not enough overlap in reads is present to produce longer and more contigs. Sequencing of these samples already turned out to be difficult and resulted in less reads than for the other samples. The reason for this is unknown, because the concentration of DNA was similar to the concentration of the dual bed top sample. To improve the results, a co-assembly of the different samples from the same filter could be made to which reads from the different heights can be mapped back to.

#### Nitrifying guilds are stratified between the filter sections, but not within them

In the analysed communities, *Bacteria* were the most abundant kingdom with 92.5% on average for all samples, while *Eukaryota*, *Archaea* and *Viruses* together represented less than 0.3%. *Bacteria* were reported before to be the main abundant kingdom in rapid sand filters (Bai et al., 2013; Gülay et al., 2016).

At phylum level, *Proteobacteria* are highly abundant (33-77 %) in all filter samples and *Nitrospirae* (3.5-38 %) follow up in most of them (Figure 3-8). Together with *Acidobacteria*, these phyla were previously found to be the main members of the community in sand filters (Albers et al., 2015; Palomo et al., 2016; Piazza et al., 2019). Low relative abundances of *Actinobacteria*, *Bacteroidetes*, *Planctomycetes* and

*Verrucomicrobia* were also observed in other rapid sand filters (Palomo et al., 2016; Poghosyan et al., 2020). These phyla are often found in fresh waters and soils, and together they are capable to perform a wide variety of functions (Madigan et al., 2015).

The ammonium removal capacity increased from the first to the second section of both filter systems (Figure 3-7) and was shown to be biotic (Figure 3-6). The relative abundance of *Nitrospirae* increased accordingly (Figure 3-8). *Nitrospirae* increased from 3.5% to 30% in the dual bed and from 8% to 22% in the sequential filter system. At genus level, the same increase in *Nitrospira* is seen: 2% to 16% in the dual bed and 6% to 11% in the sequential filters (Figure 3-9). Together with *Nitrosomonas*, these genera are considered to be the main ammonium oxidizers in rapid sand filters (Bai et al., 2013; de Vet, Kleerebezem, et al., 2011). The increase in *Nitrospirae* lineages in the second filter of other sequential filter systems was suggested as well (Gülay et al., 2016). However, higher bacterial densities were reported for the first filters of these systems, so it was difficult to prove the higher absolute abundances in the second filter (Gülay et al., 2016; Tatari et al., 2017). The high relative abundance of *Nitrospirae* in the first filter is unexpected, since iron is the main component of the coating (Figure 3-1) and nitrification was previously suggested to be hindered by iron presence (De Vet et al., 2009).

Despite absolute DNA abundances were not quantified in this study, it is reasonable to assume the total abundance of *Nitrospirae* is higher in the second sections compared to first sections. The DNA extraction yields provide an indication for the number of microorganisms present on the sand. 2-3 times more DNA was found in the second section compared to the first one (Table 3.3). Besides, for the dual bed, the volume of the sand layer is three times bigger than the anthracite layer. In conclusion, more nitrifying organisms are present in the second sections, in accordance with plant profiles (Figure 3-3) and ammonium removal capacities (Figure 3-7). These results confirm the biological origin of ammonium removal in the filters.

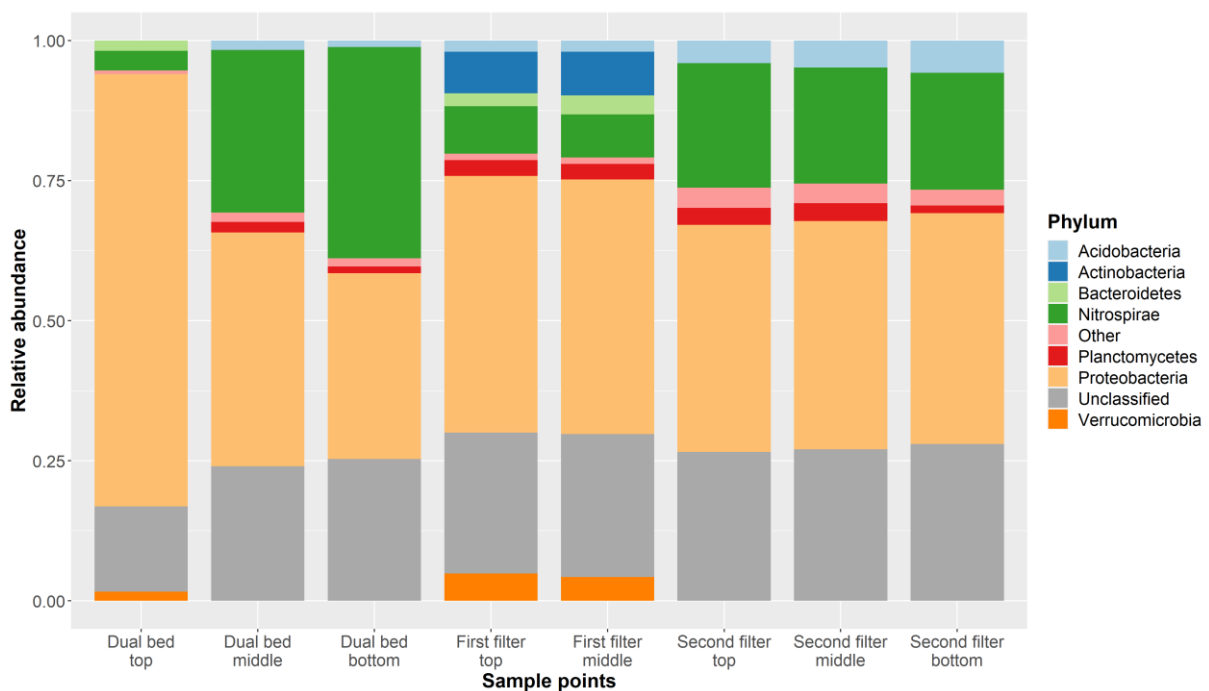


Figure 3-8. Relative abundances of phyla in all filter samples. Phyla with a relative abundance below 1% are grouped as 'Other'.

Table 3.3. DNA extraction yields for all filter bed samples before column purification.

	Dual bed			First filter		Second filter		
	Top	Middle	Bottom	Top	Middle	Top	Middle	Bottom
Extraction yield ( $\mu\text{g}_{\text{DNA}}/\text{g}_{\text{sand}}$ )	0.035	0.082	0.069	3.2	1.8	10.0	5.1	8.2

In the second filter, no stratification of *Nitrospirae* is seen in the relative abundances or the DNA extraction, while a strong stratification was observed during the batch test (Figure 3-7). It is possible that the community composition stays stable, while the absolute abundances decrease over the filter. The absolute abundance should therefore be determined with another method like qPCR or metaproteomics, to see if the stratification is visible there again. Metaproteomic analysis will be performed on all samples to study protein expression levels, but this was beyond the scope of this thesis. Most of the dry weight of cells is formed by proteins, and DNA forms a minor fraction of the cell mass (Alberts et al., 2014). Therefore, the absolute abundances obtained with proteomic analysis better reflect the amount of biomass than DNA-based absolute abundances.

### Biological removal of iron in the dual bed filter system

Besides nitrifying organisms, many more species are present in the microbial community living on the sand grains. These species perform a variety of functions within the filters, so the community was studied on a higher taxonomic level as well. In dual bed top, *Gallionella* and *Sideroxydans* appear as important genera present in the community (Figure 3-9). These are both known as iron-oxidizing bacteria (FeOB) (de Vet, Dinkla, et al., 2011; Weiss et al., 2007). The top layer of the dual bed is responsible for iron removal (Figure 3-3), so the presence of FeOB was expected in this location.

The dominance of FeOB in the dual bed indicates the importance of biological iron oxidation in the anthracite layer. On the other hand, the low the DNA extraction yield (Table 3.3) suggests a low absolute abundance. It could be that FeOB are mainly important for the removal of iron when the filter is young. When the filter matures, more iron(hydr)oxides are present on the sand to act as catalyst in the chemical oxidation of iron. A similar idea was suggested for the removal of manganese: biological processes are responsible during start-up and chemical processes take over when the filter matures (Bruins et al., 2015). However, the coating of the anthracite layer contains a significant amount of iron (Figure 3-1). This indicates a significant amount of iron(hydr)oxides is already present on the grains, thus the chemical oxidation of iron might still be more important in the filter.

The concurrent presence of FeOB and nitrifying organisms is in contrast with the common idea that iron oxidation has to be complete before the start of ammonium oxidation (Mouchet, 1992; Tekerlekopoulou et al., 2013). The nitrifying organisms are not only present, but also active as shown by the nitrifying activity in both the batch test (Figure 3-7) and the filter (Figure 3-3). No activity test was performed to verify the biological  $\text{Fe}^{2+}$  removal capacity of the sand, but the metaproteomic analysis will provide information about the activity of the FeOB. To conclude, we suggest biological removal of iron and ammonium can take place simultaneously and biological iron removal might be significantly important in the anthracite layer of the dual bed. The metaproteomic analysis will provide more information to obtain a better understanding of the FeOB in the filter system.

## The presence of other functionalities in the filters

Minor members of the community can play important roles in the removal of other contaminants or the production of substrates for the other microorganisms present. The microbial communities of the first filter sections seem more diverse than the communities of the second sections (Figure 3-9). The first section consists of at least six genera, while the second section mainly consists of nitrifiers. This observation is in contrast with another study reporting an increase in diversity in the second filter of two plants and a similar diversity of the two filters in two other plants (Gülay et al., 2016). The completely different observations show more research is required to understand what the degree of diversity tells about the functioning of the filter.

Typical manganese-oxidizing bacteria (MnOB) like *Leptotrix* spp. and *Pseudomonas* spp. were not detected, while they were found in rapid sand filters before (Burger et al., 2008; Piazza et al., 2019). This indicates manganese removal in the filter is mainly chemical, but it could also be that yet unknown MnOB are present.

The function of *Hyphomicrobium* in rapid sand filters is not understood yet. Species belonging to this genus were shown to be methanol-dependent denitrifiers, but studies also speculated about a potential role in the oxidation of manganese (Albers et al., 2015; Martineau et al., 2015). *Methyloglobulus* and *Methylotenera* are methane-oxidizers, so their presence indicates the raw water contains methane (Albers et al., 2015; Poghosyan et al., 2020). The genus *Archangium* has mainly been found in soil and consumes insoluble organic substances like starch (Lang et al., 2015). *Chthoniobacter* is an aerobic heterotroph, belonging to the phylum *Verrucomicrobia* (Sangwan et al., 2004).

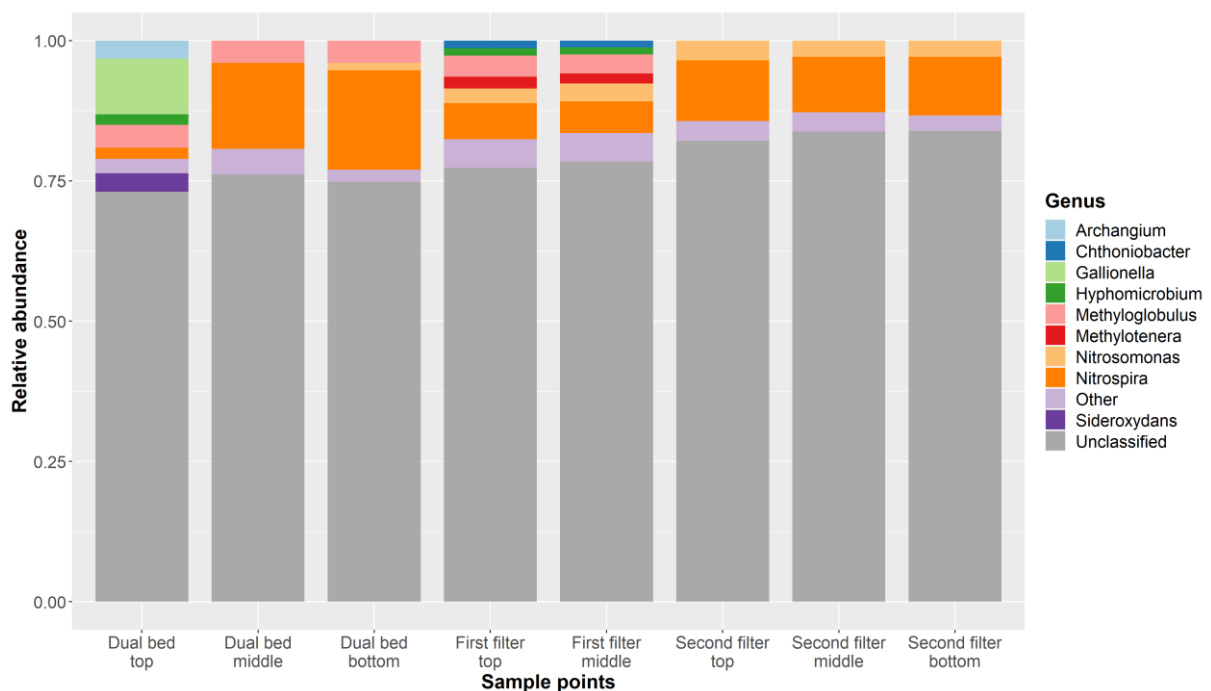


Figure 3-9. Relative abundances of genera in all filter samples. Genera with a relative abundance below 1% are grouped as 'Other'.

## 4. Conclusions

In the present work, the stratification of  $\text{Fe}^{2+}$ ,  $\text{NH}_4^+$  and  $\text{Mn}^{2+}$  removal processes in rapid sand filters was investigated. Specifically, we focused on quantitatively resolving the contribution and spatial distribution of the microbiological and physicochemical removal mechanisms responsible for such observed stratification. To do so, three full-scale rapid sand filters from two DWTPs with different plant configuration but comparable incoming water compositions were investigated. One of the plants uses one dual bed, while the other plant uses two sequential filters. Water samples and filter bed material from both plants were analysed. Concentration profiles and coating composition showed the removal location of each contaminant. Furthermore, activity batch test were used to characterize the removal mechanisms at different heights. Lastly, metagenomic analysis was performed on all filter bed samples to study the composition of the microbial community in the different locations. Based on the obtained results, several conclusions can be drawn.

Regardless of the configuration (1 or 2 RSF), the plants could be divided in two sections. In the first one, iron(hydr)oxides dominate the coating and ammonium and iron are oxidized. In the second one, manganese oxides are the dominant component of the coating, and ammonium and manganese are oxidized. Multiple analysis supported the division into sections: the composition of the coating, concentration profiles over the plant, removal mechanisms and capacity of ammonium and manganese and the distribution of the microbial community.

This conclusion is supported by the following observations:

- The removal of  $\text{Fe}^{2+}$  and  $\text{Mn}^{2+}$  takes place in separate filter sections, while  $\text{NH}_4^+$  is removed throughout both of them. During filtration, grains in the first and second section are covered with iron(hydr)oxides and manganese oxides respectively.
- Anthracite penetration into the sand layer results in iron presence in the second part of the dual bed. The presence of iron diminishes the manganese oxidation capacity of the second part, since iron(hydr)oxides do not act as a catalyst in the oxidation of manganese. Moreover, nitrification capacity might be hindered by the presence of iron.
- The two filter sections show different manganese removal mechanisms: adsorption and oxidation respectively. For the very first time, we proved aerobic manganese removal through adsorption on iron(hydr)oxides. In the full-scale process, manganese removal is dominated by oxidation.
- Ammonium removal is carried out exclusively by nitrifying organisms. The nitrification capacity is stratified over the height of the filter bed. The relative abundance of nitrifying guilds is stratified between the filter sections, but not within the sections.
- Manganese oxidation capacity remains constant over the filter height, while the removal capacity of ammonium is stratified. We propose two hypothesis to explain this difference. One explanation is based on the biological origin of ammonium removal. Microorganisms quickly adapt to different conditions, such as experiencing lower ammonium concentrations due to mixing during backwashing. On the other hand, manganese oxides act as a catalyst in the oxidation of manganese and their presence does not change upon experiencing different conditions.

## 5. Recommendations for further work

- I. To better understand the implications of the observed division into two sections, future studies should address the effect of using dual bed or sequential filter systems on process operation capacity, cost efficiency and long-term stability. Similar processes are responsible for the removal of contaminants, but anthracite penetration might have large consequences on the performance of the dual bed.
- II. Oxidation is the dominant process for the removal of manganese in the filter. The oxidation capacity remains constant over the height, while a stratified removal was expected. We hypothesize that the capacity remains constant, because the available area of manganese oxides is constant over the filter bed. To study the correlation between the oxidation capacity and the available area of oxides, batch tests using sand containing different amounts of available manganese oxides should be performed.
- III. The ammonium removal rates observed in the filter are lower than the rates observed in the batch test. Optimization of the process conditions, such as the addition of phosphate (De Vet et al., 2012), could therefore result in more efficient ammonium removal.
- IV. Metagenomic analysis of the microbiome from rapid sand filters is challenging due to the low amounts of biomass and the diversity of the microbial community. Long read sequencing should be used to ease the assembly of longer contigs and binning, which is required to study the presence of functions in a (group) of organisms. Co-assembling the reads originating from different heights within one filter should also be tried. Using the co-assembly for the taxonomic analysis might increase the amount of contigs that can be annotated.
- V. Functional annotation should be performed on the metagenomic data obtained in this study to investigate the metabolic potential of the RSF community. In combination with metaproteomics, this information will provide a quantitative analysis of the metabolic potential of the microbial community, which can be linked to the full-scale removal rates.

## 6. References

- 3500-Fe IRON. (n.d.). *Standard Methods For the Examination of Water and Wastewater*. <https://doi.org/10.2105/SMWW.2882.055>
- Albers, C. N., Ellegaard-Jensen, L., Harder, C. B., Rosendahl, S., Knudsen, B. E., Ekelund, F., & Aamand, J. (2015). Groundwater chemistry determines the prokaryotic community structure of waterworks sand filters. *Environmental Science and Technology*, 49(2), 839–846. <https://doi.org/10.1021/es5046452>
- Alberts, B., Johnson, A., Walter, P., Raff, M., Lewis, J., & Roberts, K. (2014). *Molecular Biology of the Cell* (6th ed.). Ww Norton & Co.
- Bai, Y., Liu, R., Liang, J., & Qu, J. (2013). Integrated Metagenomic and Physicochemical Analyses to Evaluate the Potential Role of Microbes in the Sand Filter of a Drinking Water Treatment System. *PLoS ONE*, 8(4). <https://doi.org/10.1371/journal.pone.0061011>
- Belser, L. W., & Mays, E. L. (1982). Use of Nitrifier Activity Measurements To Estimate the Efficiency of Viable Nitrifier Counts in Soils and Sediments. *Applied and Environmental Microbiology*, 43(4), 945–948. <https://doi.org/10.1128/aem.43.4.945-948.1982>
- Breda, I. L., Ramsay, L., Søbørg, D. A., Dimitrova, R., & Roslev, P. (2019). Manganese removal processes at 10 groundwater fed full-scale drinking water treatment plants. *Water Quality Research Journal of Canada*, 54(4). <https://doi.org/10.2166/wqrj.2019.006>
- Bruins, J. (2017). Manganese removal from groundwater: Role of biological and physico-chemical autocatalytic processes. In *Manganese Removal from Groundwater: Role of Biological and Physico-Chemical Autocatalytic Processes*. <https://doi.org/10.1201/9781315115900>
- Bruins, J. H., Petrusevski, B., Slokar, Y. M., Huysman, K., Joris, K., Kruithof, J. C., & Kennedy, M. D. (2015). Biological and physico-chemical formation of Birnessite during the ripening of manganese removal filters. *Water Research*, 69. <https://doi.org/10.1016/j.watres.2014.11.019>
- Brunauer, S., Emmett, P. H., & Teller, E. (1938). Adsorption of Gases in Multimolecular Layers. *Journal of the American Chemical Society*, 60(2), 309–319. <https://doi.org/10.1021/ja01269a023>
- Buamah, R., Petrusevski, B., & Schippers, J. C. (2008). Adsorptive removal of manganese(II) from the aqueous phase using iron oxide coated sand. *Journal of Water Supply: Research and Technology - AQUA*, 57(1), 1–11. <https://doi.org/10.2166/aqua.2008.078>
- Burger, M. S., Krentz, C. A., Mercer, S. S., & Gagnon, G. A. (2008). Manganese removal and occurrence of manganese oxidizing bacteria in full-scale biofilters. *Journal of Water Supply: Research and Technology - AQUA*, 57(5), 351–359. <https://doi.org/10.2166/aqua.2008.050>
- Cai, Y., Li, D., Liang, Y., Luo, Y., Zeng, H., & Zhang, J. (2015). Effective start-up biofiltration method for Fe, Mn, and ammonia removal and bacterial community analysis. *Bioresource Technology*, 176, 149–155. <https://doi.org/10.1016/j.biortech.2014.11.025>
- Cerrato, J. M., Falkinham, J. O., Dietrich, A. M., Knocke, W. R., McKinney, C. W., & Pruden, A. (2010). Manganese-oxidizing and -reducing microorganisms isolated from biofilms in chlorinated drinking water systems. *Water Research*, 44(13), 3935–3945. <https://doi.org/10.1016/j.watres.2010.04.037>

- Cheng, Q., Nengzi, L., Xu, D., Guo, J., & Yu, J. (2017). Influence of nitrite on the removal of Mn(II) using pilot-scale biofilters. *Journal of Water Reuse and Desalination*, 7(3), 264–271. <https://doi.org/10.2166/wrd.2016.210>
- Claff, S. R., Sullivan, L. A., Burton, E. D., & Bush, R. T. (2010). A sequential extraction procedure for acid sulfate soils: Partitioning of iron. *Geoderma*, 155(3–4), 224–230. <https://doi.org/10.1016/j.geoderma.2009.12.002>
- Daims, H., Lebedeva, E. V., Pjevac, P., Han, P., Herbold, C., Albertsen, M., Jehmlich, N., Palatinszky, M., Vierheilig, J., Bulaev, A., Kirkegaard, R. H., Von Bergen, M., Rattei, T., Bendinger, B., Nielsen, P. H., & Wagner, M. (2015). Complete nitrification by *Nitrospira* bacteria. *Nature*, 528(7583), 504–509. <https://doi.org/10.1038/nature16461>
- Davies, S. H. R., & Morgan, J. J. (1989). Manganese(II) oxidation kinetics on metal oxide surfaces. *Journal of Colloid And Interface Science*, 129(1), 63–77. [https://doi.org/10.1016/0021-9797\(89\)90416-5](https://doi.org/10.1016/0021-9797(89)90416-5)
- Davison, W., & Seed, G. (1983). The kinetics of the oxidation of ferrous iron in synthetic and natural waters. *Geochimica et Cosmochimica Acta*, 47(1), 67–79. [https://doi.org/10.1016/0016-7037\(83\)90091-1](https://doi.org/10.1016/0016-7037(83)90091-1)
- de Vet, W. W. J. M., Dinkla, I. J. T., Muyzer, G., Rietveld, L. C., & van Loosdrecht, M. C. M. (2009). Molecular characterization of microbial populations in groundwater sources and sand filters for drinking water production. *Water Research*, 43(1), 182–194. <https://doi.org/10.1016/j.watres.2008.09.038>
- de Vet, W. W. J. M., Dinkla, I. J. T., Rietveld, L. C., & van Loosdrecht, M. C. M. (2011). Biological iron oxidation by *Gallionella* spp. in drinking water production under fully aerated conditions. *Water Research*, 45(17), 5389–5398. <https://doi.org/10.1016/j.watres.2011.07.028>
- de Vet, W. W. J. M., Kleerebezem, R., van der Wielen, P. W. J. J., Rietveld, L. C., & van Loosdrecht, M. C. M. (2011). Assessment of nitrification in groundwater filters for drinking water production by qPCR and activity measurement. *Water Research*, 45(13), 4008–4018. <https://doi.org/10.1016/j.watres.2011.05.005>
- De Vet, W. W. J. M., Rietveld, L. C., & Van Loosdrecht, M. C. M. (2009). Influence of iron on nitrification in full-scale drinking water trickling filters. *Journal of Water Supply: Research and Technology - AQUA*, 58(4), 247–256. <https://doi.org/10.2166/aqua.2009.115>
- De Vet, W. W. J. M., Van Loosdrecht, M. C. M., & Rietveld, L. C. (2012). Phosphorus limitation in nitrifying groundwater filters. *Water Research*, 46(4), 1061–1069. <https://doi.org/10.1016/j.watres.2011.11.075>
- Geudens, P. J. J. ., & Grootveld, J. (2017). Dutch Drinking Water Statistics 2017. *Association of Dutch Water Companies (Vewin), Den Haag*, 130. <https://www.vewin.nl/SiteCollectionDocuments/Publicaties/Cijfers/Drinkwaterstatistieken-2017-EN.pdf>
- Gouzinis, A., Kosmidis, N., Vayenas, D. V., & Lyberatos, G. (1998). Removal of Mn and Simultaneous Removal of NH<sub>3</sub>, Fe and Mn from Potable Water using a Trickling Filter. *Water Research*, 32(8), 2442–2450.
- Gude, J. C. J., Rietveld, L. C., & van Halem, D. (2016). Fate of low arsenic concentrations during full-scale aeration and rapid filtration. *Water Research*, 88, 566–574. <https://doi.org/10.1016/j.watres.2015.10.034>

- Gülay, A., Musovic, S., Albrechtsen, H. J., Al-Soud, W. A., Sørensen, S. J., & Smets, B. F. (2016). Ecological patterns, diversity and core taxa of microbial communities in groundwater-fed rapid gravity filters. *ISME Journal*, *10*(9), 2209–2222. <https://doi.org/10.1038/ismej.2016.16>
- Gülay, A., Tatari, K., Musovic, S., Mateiu, R. V., Albrechtsen, H. J., & Smets, B. F. (2014). Internal porosity of mineral coating supports microbial activity in rapid sand filters for groundwater treatment. *Applied and Environmental Microbiology*, *80*(22), 7010–7020. <https://doi.org/10.1128/AEM.01959-14>
- Guo, Y., Huang, T., Wen, G., & Cao, X. (2017). The simultaneous removal of ammonium and manganese from groundwater by iron-manganese co-oxide filter film: The role of chemical catalytic oxidation for ammonium removal. *Chemical Engineering Journal*, *308*, 322–329. <https://doi.org/10.1016/j.cej.2016.09.073>
- Katsoyiannis, I. A., & Zouboulis, A. I. (2004). Biological treatment of Mn(II) and Fe(II) containing groundwater: Kinetic considerations and product characterization. *Water Research*, *38*(7), 1922–1932. <https://doi.org/10.1016/j.watres.2004.01.014>
- Lang, E., Schumann, P., Tindall, B. J., Mohr, K. I., & Spröer, C. (2015). Reclassification of *Angiococcus disciformis*, *Cystobacter minus* and *Cystobacter violaceus* as *Archangium disciforme* comb. nov., *Archangium minus* comb. nov. and *Archangium violaceum* comb. nov., Unification of the families Archangiaceae and Cystobacteraceae. *International Journal of Systematic and Evolutionary Microbiology*, *65*(11), 4032–4042. <https://doi.org/10.1099/ijsem.0.000533>
- Lee, C. O., Boe-Hansen, R., Musovic, S., Smets, B., Albrechtsen, H. J., & Binning, P. (2014). Effects of dynamic operating conditions on nitrification in biological rapid sand filters for drinking water treatment. *Water Research*, *64*(m), 226–236. <https://doi.org/10.1016/j.watres.2014.07.001>
- Madigan, M., Martinko, J., Bender, K., Buckley, D., & Stahl, D. (2015). *Brock Biology of Microorganisms* (14th ed.). Pearson Education.
- Martineau, C., Mauffrey, F., & Villemur, R. (2015). Comparative analysis of denitrifying activities of *Hyphomicrobium nitratorans*, *Hyphomicrobium denitrificans*, and *Hyphomicrobium zavarzinii*. *Applied and Environmental Microbiology*, *81*(15), 5003–5014. <https://doi.org/10.1128/AEM.00848-15>
- Mouchet, P. (1992). From conventional to biological removal of iron and manganese in France. *Journal / American Water Works Association*, *84*(4), 158–167. <https://doi.org/10.1002/j.1551-8833.1992.tb07342.x>
- Olańczuk-Neyman, K., Olańczuk-Neyman, K., & Bray, R. (2000). The Role of Physico-Chemical and Biological Processes in Manganese and Ammonia Nitrogen Removal from Groundwater. *Polish Journal of Environmental Studies*, *9*(2), 91–96. <https://www.researchgate.net/publication/288170604>
- Palomo, A., Jane Fowler, S., Gülay, A., Rasmussen, S., Sicheritz-Ponten, T., & Smets, B. F. (2016). Metagenomic analysis of rapid gravity sand filter microbial communities suggests novel physiology of *Nitrospira* spp. *ISME Journal*, *10*(11), 2569–2581. <https://doi.org/10.1038/ismej.2016.63>
- Pharand, L., Van Dyke, M. I., Anderson, W. B., & Huck, P. M. (2014). Assessment of biomass in drinking water Biofilters by Adenosine triphosphate. *Journal - American Water Works Association*, *106*(10), E433–E444. <https://doi.org/10.5942/jawwa.2014.106.0107>
- Piazza, A., Casalini, L. C., Pacini, V. A., Sanguinetti, G., Ottado, J., & Gottig, N. (2019). Environmental bacteria involved in manganese(II) oxidation and removal from groundwater. *Frontiers in Microbiology*, *10*(FEB). <https://doi.org/10.3389/fmicb.2019.00119>

- Poghosyan, L., Koch, H., Frank, J., van Kessel, M. A. H. J., Cremers, G., van Alen, T., Jetten, M. S. M., Op den Camp, H. J. M., & Lücker, S. (2020). Metagenomic profiling of ammonia- and methane-oxidizing microorganisms in two sequential rapid sand filters. *Water Research*, *185*. <https://doi.org/10.1016/j.watres.2020.116288>
- Sahabi, D. M., Takeda, M., Suzuki, I., & Koizumi, J. ichi. (2009). Removal of Mn<sup>2+</sup> from water by “aged” biofilter media: The role of catalytic oxides layers. *Journal of Bioscience and Bioengineering*, *107*(2), 151–157. <https://doi.org/10.1016/j.jbiosc.2008.10.013>
- Sangwan, P., Chen, X., Hugenholtz, P., & Janssen, P. H. (2004). Chthoniobacter flavus gen. nov., sp. nov., the first pure-culture representative of subdivision two, Spartobacteria classis nov., of the phylum Verrucomicrobia. *Applied and Environmental Microbiology*, *70*(10), 5875–5881. <https://doi.org/10.1128/AEM.70.10.5875-5881.2004>
- Schoonenberg, F. (n.d.). *Personal communication*.
- Shi, P., Jia, S., Zhang, X. X., Zhang, T., Cheng, S., & Li, A. (2013). Metagenomic insights into chlorination effects on microbial antibiotic resistance in drinking water. *Water Research*, *47*(1), 111–120. <https://doi.org/10.1016/j.watres.2012.09.046>
- Sung, W., & Morgan, J. J. (1980). Kinetics and Product of Ferrous Iron Oxygenation in Aqueous Systems. *Environmental Science & Technology*, *14*(5), 561–568.
- Tatari, K., Smets, B. F., & Albrechtsen, H. J. (2016). Depth investigation of rapid sand filters for drinking water production reveals strong stratification in nitrification biokinetic behavior. *Water Research*, *101*, 402–410. <https://doi.org/10.1016/j.watres.2016.04.073>
- Tatari, Karolina, Musovic, S., Gülay, A., Dechesne, A., Albrechtsen, H. J., & Smets, B. F. (2017). Density and distribution of nitrifying guilds in rapid sand filters for drinking water production: Dominance of Nitrospira spp. *Water Research*, *127*, 239–248. <https://doi.org/10.1016/j.watres.2017.10.023>
- Tekerlekopoulou, A. G., Pavlou, S., & Vayenas, D. V. (2013). Removal of ammonium, iron and manganese from potable water in biofiltration units: A review. In *Journal of Chemical Technology and Biotechnology* (Vol. 88, Issue 5, pp. 751–773). <https://doi.org/10.1002/jctb.4031>
- Van Beek, C. G. E. M., Hiemstra, T., Hofs, B., Nederlof, M. M., Van Paassen, J. A. M., & Reijnen, G. K. (2012). Homogeneous, heterogeneous and biological oxidation of iron(II) in rapid sand filtration. *Journal of Water Supply: Research and Technology - AQUA*, *61*(1), 1–13. <https://doi.org/10.2166/aqua.2012.033>
- van den Akker, B., Holmes, M., Cromar, N., & Fallowfield, H. (2008). Application of high rate nitrifying trickling filters for potable water treatment. *Water Research*, *42*(17), 4514–4524. <https://doi.org/10.1016/j.watres.2008.07.038>
- van Dijk, H. J. C., Verberk, J. Q. J. C., & de Moel, P. J. (2006). *Drinking water: principles and practices*. World Scientific Publishing Company.
- Van Kessel, M. A. H. J., Speth, D. R., Albertsen, M., Nielsen, P. H., Op Den Camp, H. J. M., Kartal, B., Jetten, M. S. M., & Lücker, S. (2015). Complete nitrification by a single microorganism. *Nature*, *528*(7583), 555–559. <https://doi.org/10.1038/nature16459>
- Vandenabeele, J., Woestyne, M. Vande, Houwen, F., Germonpr, R., Vandesande, D., & Verstraete, W. (1995). Role of Autotrophic Nitrifiers in Biological Manganese Removal from Groundwater Containing Manganese and Ammonium. *Microbial Ecology*, *29*, 83–98.

- Vries, D., Bertelkamp, C., Schoonenberg Kegel, F., Hofs, B., Dusseldorp, J., Bruins, J. H., de Vet, W., & van den Akker, B. (2017). Iron and manganese removal: Recent advances in modelling treatment efficiency by rapid sand filtration. *Water Research*, 109. <https://doi.org/10.1016/j.watres.2016.11.032>
- Yang, H., Yan, Z., Du, X., Bai, L., Yu, H., Ding, A., Li, G., Liang, H., & Aminabhavi, T. M. (2020). Removal of manganese from groundwater in the ripened sand filtration: Biological oxidation versus chemical auto-catalytic oxidation. *Chemical Engineering Journal*, 382. <https://doi.org/10.1016/j.cej.2019.123033>

## 7. Appendices

### I. Protocol to prepare trace element solution

Trace element solution was prepared using this protocol.

- 1) Suspend EDTA and  $\text{ZnSO}_4 \cdot 7\text{H}_2\text{O}$  in 3.75 L demi water and adjust pH to 6.0 using NaOH (p.a).
- 2) Dissolve the rest of the chemicals one by one in the described order. Keep the pH at 6.0. Wait until a chemical is completely dissolved and medium is clear before adding another chemical.

Table I. Composition of trace element solution.

Chemical	Chemical formula	Concentration ( $\text{g L}^{-1}$ )
EDTA (Titriplex III®)	$\text{C}_{10}\text{H}_{14}\text{N}_2\text{Na}_2\text{O}_8 \cdot 2\text{H}_2\text{O}$	15.00
Zink sulfate. $7\text{H}_2\text{O}$	$\text{ZnSO}_4 \cdot 7\text{H}_2\text{O}$	4.50
Manganese chloride. $2\text{H}_2\text{O}$	$\text{MnCl}_2 \cdot 2\text{H}_2\text{O}$	0.84
Cobalt(II)chloride. $6\text{H}_2\text{O}$ (Toxic)	$\text{CoCl}_2 \cdot 6\text{H}_2\text{O}$	0.30
Copper (II) sulfate. $5\text{H}_2\text{O}$	$\text{CuSO}_4 \cdot 5\text{H}_2\text{O}$	0.30
Sodium molybdenum. $2\text{H}_2\text{O}$	$\text{Na}_2\text{MoO}_4 \cdot 2\text{H}_2\text{O}$	0.40
Calciumchloride. $2\text{H}_2\text{O}$	$\text{CaCl}_2 \cdot 2\text{H}_2\text{O}$	4.50
Iron sulfate. $7\text{H}_2\text{O}$	$\text{FeSO}_4 \cdot 7\text{H}_2\text{O}$	3.00
Boron acid	$\text{H}_3\text{BO}_3$	1.00
Potassium iodide	KI	0.10

- 3) Adjust the pH to 4.0 using HCl 1M and add demi water until a final volume of 5 L.
- 4) Sterilize for 20 min. at  $121^\circ\text{C}$ .

## II. Physical characteristics of the filter bed material

The specific surface area of the sand grains was estimated using the Brunauer-Emmet-Teller (BET) theory (Bolger et al., 2014). Freeze-dried sand was degassed for 16 hours at 60°C in vacuum ( $p < 0.15$  mbar) (VacPrep 061, Micromeritics, USA). The specific surface area was estimated using a surface area and porosity analyzer (Tristar II, Micromeritics, USA). Helium was used to determine the volume of the open space above the sample. The adsorption and desorption isotherms were measured by N<sub>2</sub> sparging. The density was determined in triplicate using the Archimedes principle: the mass and volume difference was followed in a measuring cylinder during the addition of wet sand. The physical characteristics of the different filter bed samples are shown in Table II.

Table II. Surface area and density of the filter bed material samples at the different sampling locations. The density is given with the standard deviation resulting from triplicate measurements.

Filter	Location	Material	BET surface area (m <sup>2</sup> g <sup>-1</sup> )	Surface area outside pores ≥ 2 nm (m <sup>2</sup> g <sup>-1</sup> )	Density (g cm <sup>-3</sup> )
Dual bed	Top	Anthracite	38	8.2	1.28 ± 0.02
Dual bed	Middle	Sand	15	4.6	1.69 ± 0.02
Dual bed	Bottom	Sand	6.7	3.1	1.72 ± 0.01
First filter	Top	Sand	19	9.7	1.73 ± 0.04
First filter	Middle	Sand	22	11	1.67 ± 0.03
Second filter	Top	Sand	3.5	2.8	1.68 ± 0.04
Second filter	Middle	Sand	3.9	3.3	1.73 ± 0.04
Second filter	Bottom	Sand	3.1	2.7	1.77 0.03

### III. Concentration profiles over dual bed

A detailed concentration profile was measured over the height of the dual bed filter. Two-third of the iron is removed in the supernatant and the first centimetres of the anthracite layer (Figure III), due to homogenous iron oxidation in the presence of oxygen (Davison & Seed, 1983). The removal of manganese and ammonium only occurs within the filter bed. The removal of ammonium and manganese is complete after 155 and 205 cm from the top of the supernatant respectively.

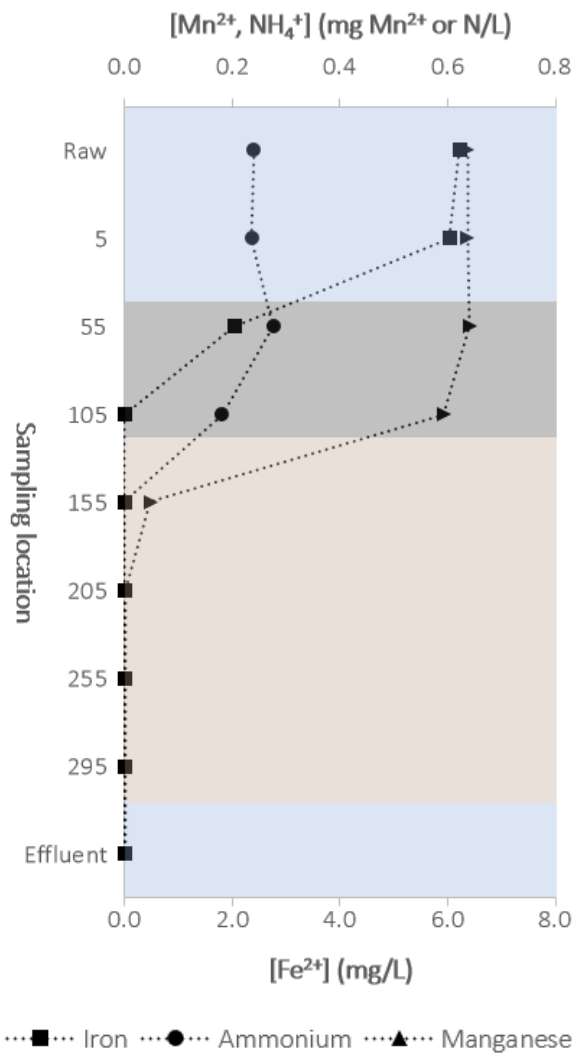


Figure III. Concentration profiles over the dual bed filter. The y-axis shows the sampling location, the numbers correspond to the distance from the top of the supernatant in cm. The colours of bed correspond to anthracite (grey) and sand (brown).



